Published online 22 June 2021

Nucleic Acids Research, 2021, Vol. 49, No. 16 ***e94***
https://doi.org/10.1093/nar/gkab521

A transferrable and integrative type I-F Cascade for heterologous genome editing and transcription modulation

Zeling Xu[1,2], Yanran Li[1], Huiluo Cao[3], Meiru Si[1,4], Guangming Zhang[1], Patrick C.Y. Woo[3] and Aixin Yan[1,*]

[1]School of Biological Sciences, The University of Hong Kong, Pokfulam Road, Hong Kong SAR, China, [2]Integrative Microbiology Research Centre, South China Agricultural University, Guangzhou, Guangdong, China, [3]Department of Microbiology, Li Ka Shing Faculty of Medicine, The University of Hong Kong, Hong Kong SAR, China and [4]School of Biological Sciences, Qufu Normal University, Qufu, Shandong, China

Received February 03, 2021; Revised May 18, 2021; Editorial Decision June 01, 2021; Accepted June 05, 2021

ABSTRACT

The Class 1 type I CRISPR–Cas systems represent the most abundant and diverse CRISPR systems in nature. However, their applications for generic genome editing have been hindered due to difficulties of introducing the class-specific, multi-component effectors (Cascade) in heterologous hosts for functioning. Here we established a transferrable Cascade system that enables stable integration and expression of a highly active type I-F Cascade in heterologous bacterial hosts for various genetic exploitations. Using the genetically recalcitrant *Pseudomonas* species as a paradigm, we show that the transferred Cascade displayed substantially higher DNA interference activity and greater editing capacity than both the integrative and plasmid-borne Cas9 systems, and enabled deletion of large fragments such as the 21-kb integrated cassette with efficiency and simplicity. An advanced I-F-λ_{red} system was further developed to enable editing in genotypes with poor homologous recombination capacity, clinical isolates lacking sequence information, and cells containing anti-CRISPR elements Acrs. Lastly, an 'all-in-one' I-F Cascade-mediated CRISPRi platform was developed for transcription modulation by simultaneous introduction of the Cascade and the programmed mini-CRISPR array in one-step. This study provides a framework for expanding the diverse type I Cascades for widespread, heterologous genome editing and establishment of editing techniques in 'non-model' bacterial species.

INTRODUCTION

Clustered regularly interspaced short palindromic repeats (CRISPR) and CRISPR-associated proteins (Cas) constitute the adaptive immune system in prokaryotes that defends against foreign genetic elements via RNA-guided nucleic acids destruction (1,2). Genome editing and therapeutic applications have focused on the Class 2 CRISPR–Cas systems owing to their simple requirement of a single, multifunctional effector, for example Cas9 and Cas12a, for DNA interference (3,4). However, Class 2 systems represent only ∼10% of the CRISPR–Cas systems encoded naturally in prokaryotes (5). Their applications to edit bacterial genomes have been frequently impeded by the poor transformation and cytotoxicity caused by heterologous expression of the large Cas9/Cas12a proteins and the requirement of species-specific optimization (6–8). In contrast to the rapid rise and extension of the tools in eukaryotes, thus far, the Cas9/Cas12a-based genome editing is only successfully established in a few model bacterial strains. A predominant, CRISPR-based editing strategy readily applicable in diverse bacterial species is lacking.

Remarkably, nearly 50% of bacteria and 90% of archaea genomes encode native CRISPR–Cas systems and 90% of these naturally occurring CRISPR–Cas systems belongs to the Class 1 systems which target invading nucleic acids via a multi-component effector complex termed as Cascade (CRISPR-associated complex for antiviral defense) (9,10). Although the complexity of these effectors has somewhat hindered their widespread application in eukaryotes, their prevalence and diversity, especially the Class 1 type I systems which account for 50% of all CRISPR–Cas systems identified with seven subtypes (i.e. I-A to I-F plus I-U), has opened new avenues for developing genome editing tools through directly repurposing the endogenous CRISPR–Cas systems in bacteria and archaea (11). The approach operates by simply delivering a programmed mini-CRISPR ar-

*To whom correspondence should be addressed. Tel: +852 22990864; Fax: +852 25599114; Email: ayan8@hku.hk

ray and a desired repair donor, which are frequently assembled in a single plasmid, into prokaryotic cells, enabling genome editing with simplicity and efficiency. Employing the strategy, editing of several genetically recalcitrant organisms such as the industrial bacterium *Clostridium pasteurianum* ATCC6013 (type I-B) (12), the clinical multidrug resistant *Pseudomonas aeruginosa* genotype PA154197 (type I-F) (13), and a human microbiome *Lactobacillus crispatus* NCK1350 (Type I-E) (14) has been achieved. Furthermore, the processive DNA degradation fashion of the type I signature nuclease Cas3 has enabled long-range genomic deletions in both bacteria (employing the Type I-C Cascade from *P. aeruginosa*) (15) and human embryonic stem cells (employing the Type I-E Cascade from *T. fusca*) (16) which are inaccessible by the Class 2 effectors. Recently, the type I-B, type I-E, and type I-F systems have also been repurposed for transcription modulation in human cells (17,18). In all these applications, the type I Cascade-mediated editing has displayed distinctive advantages, such as high specificity, minimal off-target, and strain stability.

Despite these advantages, currently, the type I CRISPR–Cas-based genome editing is limited to a subset of microbial hosts that harbor a functionally characterized and highly active endogenous CRISPR–Cas system. However, ∼50% of bacterial genomes are CRISPR-free and a significant portion of natural CRISPR–Cas systems are found to be degenerated without DNA targeting and interference activities (19,20), hindering the widespread application of the endogenous type I Cascade-mediated editing. To overcome this barrier, in this study, we developed a transferrable type I CRISPR–Cas system which enables stable integration and expression of a functional type I Cascade in heterologous bacterial hosts for diverse genetic exploitations. We employ the type I-F Cascade to demonstrate the applications since the subtype represents a relatively small size and simple architecture than most other type I systems due to the presence of a single DNA-recognizing subunit *cas8f* and the unique *cas2–cas3* gene fusion (Figure 1A) (21). Furthermore, the subtype occurs exclusively in bacterial organisms, particularly Gammaproteobacteria, underscoring its broad application potentials in this most genera-rich taxa.

The Gammaproteobacterium *Pseudomonas aeruginosa* is a primary model organism for the type I-F CRISPR–Cas system. The opportunistic pathogen is particularly notorious for its large genome size and diverse genotypes (22), rendering difficulty of establishing genetic tools in the strains of interests, especially those with clinical, environmental, or industrial significance. Hence, the species represents as a desirable model for establishing genome-editing tools and assessing their applications. To achieve transferability and stable expression of the I-F Cascade, we cloned the entire *cas* operon encoded in the previously characterized PA154197 strain in the integration-proficient vector mini-CTX and constructed the transferrable I-F system mini-CTX-IF-P*tat-lacZ*. We show that the highly active type I-F Cascade in this system is stably integrated and expressed in diverse *P. aeruginosa* genotypes following conjugation, enabling simple and efficient genetic exploitations based on the 'endogenous' CRISPR–Cas system in the transferred hosts. Furthermore, an advanced mini-CTX-IF-λ_{red}-P*tat-lacZ* system is developed to achieve genome editing in homologous recombination poor genotypes, including strains lacking genome sequence information. Following the desired genome editing, the integrated cassette (21.212 kb) encompassing the entire I-F Cascade genes, a *lacZ* reporter, and a λ-Red recombination system is readily removed by employing a common cassette-deleting editing plasmid we devised. We also show that the system is applicable in strains containing anti-CRISPR (Acr) elements following firstly removing *acr* genes by the counter selection-based approach and is readily applicable in other *Pseudomonas* species such as *P. putida*. Lastly, a I-F CRISPRi platform which lacks the nuclease Cas2–3 and is equipped with a multiple cloning site for incorporation of the programmed mini-CRISPR array is developed to enable one-step gene transcription modulation in heterologous hosts. Since integration by conjugation is a common approach for DNA transfer in bacteria including the wild isolates in their natural environments (23,24), our approach provides a framework for widespread exploitation of the diverse type I CRISPR–Cas systems for heterologous genome editing and establishment of genome editing tools in 'non-model' species.

MATERIALS AND METHODS

Plasmids, primers and bacterial growth conditions

All the bacterial strains, plasmids and primers used in this study are summarized in the Supplementary Table S1. *E. coli* DH5α was employed for plasmid propagation and was usually cultured at 37°C in lysogeny broth (LB) or on the LB agar plate supplemented with required antibiotics. *E. coli* SM10 was employed for conjugative plasmid delivery. *P. aeruginosa* clinical strains were isolated from the Queen Mary Hospital in Hong Kong, China. Antibiotics supplemented in the agar plates for culturing DH5α were 20 μg/ml kanamycin, 10 μg/ml tetracycline or 200 μg/ml ampicillin. Antibiotics supplemented in the agar plates for culturing SM10 were 500 μg/ml kanamycin, 10 μg/ml tetracycline or 200 μg/ml ampicillin. Antibiotics supplemented in the agar plates for culturing *P. aeruginosa* strains were 500 μg/ml kanamycin, 50 μg/ml tetracycline or 200 μg/ml carbenicillin.

Construction of the mini-CTX-IF-P*tat-lacZ* and mini-CTX-IF-λ_{red}-P*tat-lacZ*

The transferrable I-F Cascade system was constructed based on the mini-CTX-*lacZ* plasmid. The mini-CTX-*lacZ* plasmid was linearized by HindIII (NEB, USA) at 37°C for 4 h. The P*tat* promoter DNA fragment was obtained by PCR using the iProof High-Fidelity DNA Polymerase (Bio-Rad, USA) and PA154197 genomic DNA as the template. The fragment was ligated into the HindIII-digested mini-CTX-*lacZ* plasmid following the instruction of the ClonExpress II One Step Cloning Kit (Vazyme, China), generating mini-CTX-P*tat-lacZ*. The I-F *cas* operon including its native promoter (8.693-kb) was obtained by PCR employing PA154197 genomic DNA as the template. The DNA fragment was inserted into the KpnI site in the mini-CTX-P*tat-lacZ* which was digested with KpnI (NEB, USA) using the ClonExpress II One Step Cloning Kit, generating

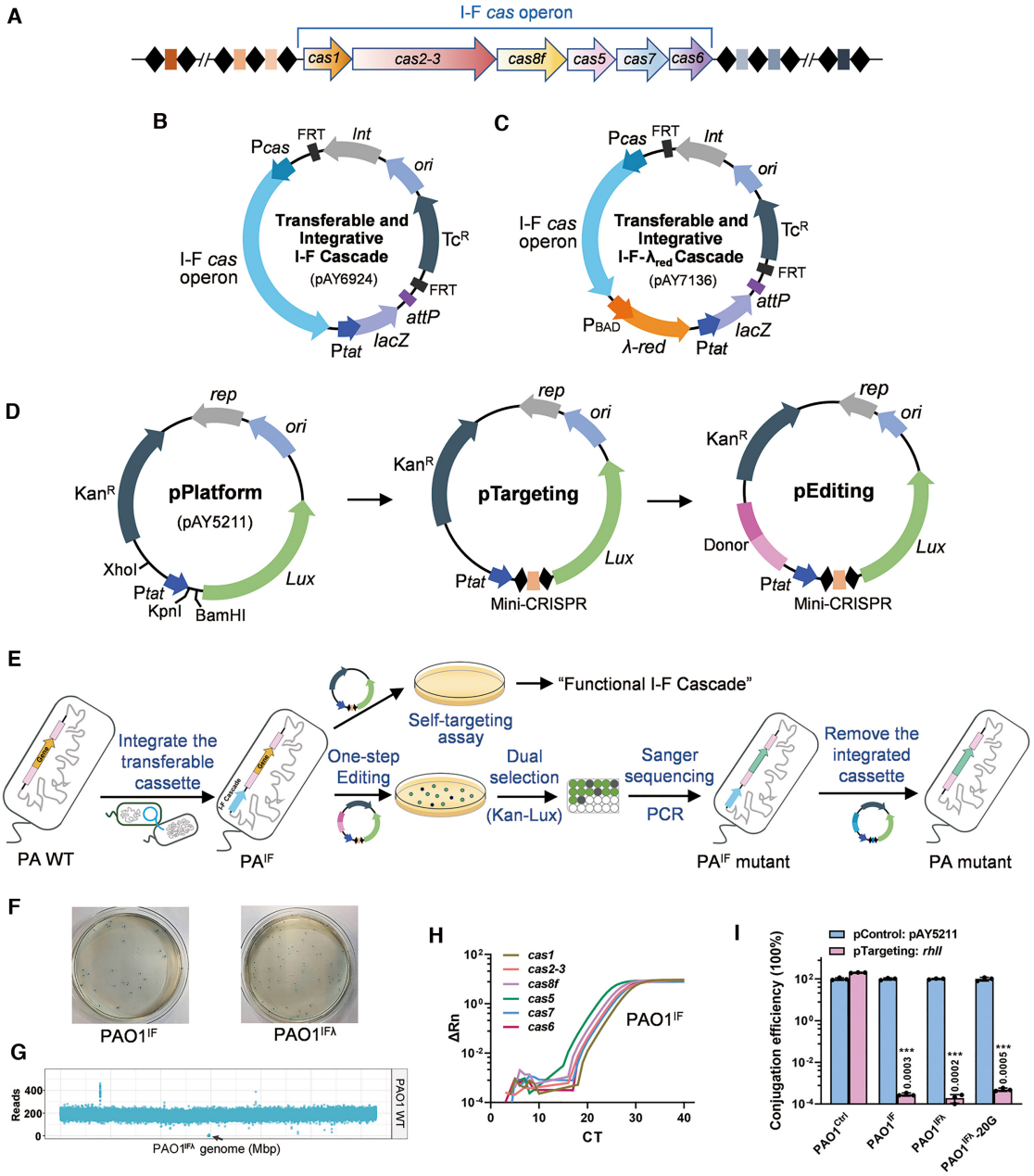

Figure 1. Overview of the transferrable and integrative type I-F Cascade-based genome editing. (**A**) Gene architecture of the type I-F *cas* operon in PA154197. (**B**) Diagram of the transferrable and integrative mini-CTX-IF-P*tat*-*lacZ* plasmid (Transferrable I-F Cascade). The organization of genes and elements in the plasmid is shown. The system contains a complete I-F *cas* operon with its native promoter from PA154197, a *lacZ* reporter gene driven by the constitutive promoter P*tat*, a fCTX integrase encoding gene *Int*, a fCTX attachment site *attP* which recognizes the chromosomal *attB* site, and two Flp recombinase target sites FRT. (**C**) Diagram of the transferrable and integrative I-F-λ_{red} Cascade. A phage λ-Red recombination system driven by P_{BAD} is assembled downstream of the I-F *cas* operon. (**D**) Assembly of the targeting plasmid (pTargeting) and editing plasmid (pEditing) for DNA interference assay and gene editing applications, respectively. (**E**) Schematic diagram showing the application of the transferrable I-F Cascade for heterologous genome editing using the *P. aeruginosa* (PA) species as an example. The transferrable I-F Cascade is firstly integrated into the *attB* site in the genome of a recipient strain (PA WT) to generate a new strain PA^{IF}. A targeting plasmid is delivered into PA^{IF} to examine the functionality of the integrated I-F Cascade. An editing plasmid is introduced to achieve desired genome editing. Recovered colonies are inoculated for luminescence-based screening. Luminescence-positive inoculum is subjected to validation by PCR and sanger sequencing. Once the desired editing is achieved, the integrated cassette is removed by another round of editing reaction employing the cassette-deleting editing plasmid (Figure 6A). (**F**) X-gal-based selection for colonies integrated with the transferrable I-F Cascade. Blue colonies indicate the successful chromosomal integration of the transferrable systems. (**G**) Mapped whole genome sequencing (WGS) reads of the PAO1 wild-type (PAO1 WT) strain against the $PAO1^{IF\lambda}$ genome. Arrow indicates the absence of reads of the integrated cassette in PAO1 WT at the *attB* site compared with $PAO1^{IF\lambda}$. (**H**) Quantitative PCR analysis of the expression of the integrated *cas* genes in $PAO1^{IF}$. Rn denotes the reporter signal normalized to the fluorescence signal of the passive reference dye (ROX). ΔRn is the value of Rn minus the baseline. (**I**) Self-targeting assay as indicated by the conjugation efficiency following introduction of the targeting and control plasmids in the indicated strains. $PAO1^{Ctrl}$: PAO1 strain integrated with the mini-CTX system lacking the *cas* operon; $PAO1^{IF}$: PAO1 strain integrated with the transferrable I-F Cascade; $PAO1^{IF\lambda}$: PAO1 strain integrated with the transferrable I-F-λ_{red} Cascade; $PAO1^{IF\lambda\text{-}20G}$: the $PAO1^{IF\lambda}$ strain after growing 20 generations in the absence of antibiotic selection. Data are displayed as mean ± SD from three biological repeats. Statistical significance is calculated based on Student's *t* test (***$P < 0.001$).

a new plasmid mini-CTX-IF-P*tat-lacZ* (Transferrable I-F Cascade, pAY6924). To construct the transferrable I-F-λ_{red} Cascade, the fragment containing the λ-Red genes and the L-arabinose inducible P_{BAD} promoter was firstly obtained by PCR employing pKD46 plasmid as the template. The fragment was inserted into the SalI sites in the mini-CTX-IF-P*tat-lacZ* using the ClonExpress II One Step Cloning Kit, generating the new plasmid mini-CTX-IF-λ_{red}-P*tat-lacZ* (Transferrable I-F-λ_{red} Cascade, pAY7136). To construct the transferrable Cas9-λ_{red} system, the I-F *cas* operon and its promoter in the transferrable I-F-λ_{red} Cascade was replaced by the Sp*cas9* gene with the P_{BAD} promoter which was amplified from pCasPA (25).

Integration of the transferrable I-F Cascade

E. coli SM10 strain transformed with the plasmid pAY6924 (transferrable I-F Cascade) was cultured in LB medium supplemented with 10 μg/ml tetracycline at 37°C with 220-rpm agitation for 16 h. Simultaneously, *P. aeruginosa* recipient strain was cultured in LB medium at 42°C with 220-rpm agitation for 16 h. Cell densities of the *E. coli* SM10 and *P. aeruginosa* cultures were determined by measuring OD_{600}. Subsequently, 1.5×10^9 CFU/ml *E. coli* SM10 and 0.25×10^9 CFU/ml *P. aeruginosa* cells were mixed and pelleted by centrifugation at 16 000 × g for 1 min. Cell pellet was re-suspended in 50 μl LB broth and subsequently spotted on the surface of a LB agar plate. Mating (plasmid delivery from SM10 to *P. aeruginosa*) occurred during the incubation of the mixture at 37°C for 8 h. Mixture was scrapped from the agar plate and resuspended in 300 μl PBS (Phosphate Buffered Saline, pH 7.4). Cell suspension was serially diluted and spread on the VBMM plates with supplementation of 50 μg/ml tetracycline and 40 μg/ml X-gal. Plates were incubated at 37°C for 24 h. Blue colonies indicating the chromosomal integration of the transferrable system were selected for further analysis.

Reverse transcription-quantitative PCR (RT-qPCR)

Expression of the integrated genes such as *cas* and λ-Red genes was examined by RT-qPCR following previous descriptions (26). Briefly, 1 ml bacterial cells cultured in LB medium were harvested when the OD_{600} reached 1.0. Total RNA was extracted employing the Takara MiniBEST Universal RNA Extraction Kit (Takara, Japan) and reverse transcription was conducted employing the PrimeScript RT Master Mix (Takara, Japan) following the manufacturer's instructions. qPCR was performed using specific primers mixed with the TB Green Premix Ex Taq (Takara, Japan) in a 20 μl reaction system. The amplification was performed in the ABI StepOnePlus real-time PCR system. Amplification curves were plotted to show the transcription levels of the genes of interest. For relative quantification of gene expression, $2^{-\Delta\Delta Ct}$ method (27) was applied and the *recA* gene was selected as the internal reference gene.

Construction of pTargeting and pEditing

A platform plasmid (pAY-mini-CRISPR, pAY6942) was firstly constructed to facilitate the construction of the desired mini-CRISPR elements required in various editing procedures. pAY6942 encompasses an insertion site encompassed by a tandem BsaI sites which are flanked by a repeat sequence (GTTCACTGCCGTATAGGCAGCTAA GAAA) specific to the I-F system at each end. A fragment of 32-bp nucleotides (N×32) preceded by a 5′-CC-3′ PAM in the coding region of the gene to be edited was firstly identified as the protospacer. Two 36-bp oligos encompassing the selected protospacer sequence flanked by four nucleotides overlapping with the 3′-end and 5′-end of the repeat sequences, i.e. 5′-GAAAN×32–3′ and 5′-GAACN×32–3′, respectively, were synthesized commercially (IDT, Singapore). The two oligos were then phosphorylated using T4 polynucleotide kinase (NEB, USA) at 37°C for 1 h. The phosphorylated oligos were heated at 95°C for 3 min and then cooled down to room temperature to generate annealed oligos. Annealed oligos were ligated into the BsaI-digested pAY6942 using the Quick LigationTM Kit (NEB, USA), resulting in a plasmid containing the desired mini-CRISPR array. Assembly of mini-CRISPR into the platform plasmid (pAY5211) results in the self-targeting plasmid (pTargeting). Further assembly of the donor template into pTargeting results in pEditing. The procedures were described previously (28). Briefly, amplified mini-CRISPR elements were digested by KpnI and BamHI (NEB, USA) and were ligated into pAY5211 employing the Quick LigationTM Kit (NEB, USA), resulting in the targeting plasmid (pTargeting). Donor sequences which usually contain the upstream and downstream homologous arms of the gene being edited with 21-bp overlap of the XhoI-digested targeting plasmid at each end were amplified by PCR and ligated into the linearized targeting plasmid (digested by XhoI (NEB, USA)) using the ClonExpress II One Step Cloning Kit (Vazyme, China), resulting in the editing plasmid (pEditing). All plasmids constructed were verified by Sanger sequencing (BGI, China).

Quantification of conjugation efficiency

E. coli SM10 strain harboring the plasmid pAY5211 or pAY7138 was cultured in LB broth supplemented with 100 μg/ml kanamycin at 37°C with 220-rpm agitation for 16 h. Simultaneously, *P. aeruginosa* strains containing the I-F or I-F-λ_{red} Cascade were cultured in LB medium at 42°C with 220-rpm agitation for 16 h. Conjugation of *E. coli* SM10 with *P. aeruginosa* was performed as described above. After conjugation, mixture was scrapped from the agar plate and resuspended in 300 μl PBS buffer. The cell suspension was subsequently adjusted to OD_{600} as 1.0 and was serially diluted and plated on the LB agar plates containing 50 μg/ml tetracycline and 500 μg/ml kanamycin (tetracycline resistance of the *P. aeruginosa* recipients due to the integrated transferrable I-F Cascade). Plates were incubated at 37°C for 24–36 h. Numbers of recovered cells from the conjugation reaction was determined by CFU obtained multiply the dilution factors. Colony number recovered from pAY5211 was set as 100%.

Genome editing and verification

E. coli SM10 strain transformed with the editing plasmid for desired gene editing was cultured in LB medium sup-

plemented with 100 μg/ml kanamycin at 37°C with 220-rpm agitation for 16 h. *P. aeruginosa* recipient strains integrated with the I-F-λ_{red} Cascade were cultured in LB medium supplemented with 20 mM L-arabinose at 42°C with 220-rpm agitation for 16 h. *P. putida* KT2440 recipient strain was cultured at 37°C. Conjugation of *E. coli* SM10 and *P. aeruginosa* or *P. putida* were performed as described above. After conjugation, the cell mixture was scrapped from the agar plate and resuspended in 300 μl PBS buffer. 150 μl cell suspension was spread on the LB agar plates containing 50 μg/ml tetracycline and 500 μg/ml kanamycin. Plates were incubated at 37°C for 24–36 h. Recovered single colonies were inoculated into LB broth containing 100 μg/ml kanamycin in a 96-well plate. After incubation at 37°C with 220-rpm agitation for 3 h, luminescence intensity was measured and ten colonies with the highest luminescence intensity were subjected to verification by colony PCR and sanger sequencing with specific primers. The editing plasmid (pEditing) in the edited *P. aeruginosa* cells was cured by streaking the cells onto a LB ager plate and incubation at 37°C for 16 h. In some cases, multiple (2 to 3) rounds of streaking are required for thorough plasmid curing. If plasmid curing by streaking is not efficient in certain genotypes, the editing plasmid can be further modified to enable target- or self-curing following the approaches described by Volke et al (29).

Bacterial whole genome sequencing and analysis

Genomic DNA was extracted from 1 ml overnight bacterial culture using the Illustra bacteria genomicPrep Mini Spin Kit (GE Healthcare, USA) according to the manufacturer's instructions. Whole genome sequencing was conducted by Novogene (Beijing, China) with the sequencing platform Novaseq. Raw reads were subjected to quality control using Trimmomatic (30). The genome of the PAO1$^{IF\lambda}$ strain was assembled using SPAdes with PAO1 (NC_002516.2) as the reference (31) and completed using an assembly improvement pipeline (32). Circlator's fixstart task was applied to fix the start position of the manually assembled complete genome of PAO1$^{IF\lambda}$ at the *dnaA* gene (33). Annotations of PAO1$^{IF\lambda}$ were conducted using Prokka with *Pseudomonas* genera specific database (34). Genome-wide integration site distribution for PAO1$^{IF\lambda}$ was conducted with the complete genome of PAO1 as the reference following previous descriptions (35). Mapping in the present study was performed using BWA (http://arXiv:1303.3997). Integration events within 500 bp bins were computed using SAMtools (36) and BEDTools (37) and visualized with ggplot2 in R platform (https://ggplot2.tidyverse.org/index.html). To explore mutations in the three PAO1$^{IF\lambda}$ Δ*rhlI* strains and three false positive strains relative to the PAO1$^{IF\lambda}$, core SNPs were collected and annotated with the PAO1$^{IF\lambda}$ genome as reference using snippy (https://github.com/tseemann/snippy).

PYO quantification

PYO production was quantified following the protocol described previously with slight modifications (38). 1 ml bacterial culture was subjected to centrifugation at 16 000 × g for 5 min. 750 μl supernatant was collected and mixed with 450 μl chloroform by vortex for 0.5 min. After centrifugation at 16 000 × g for 5 min, 400 μl liquid from lower phase was then mixed with 200 μl HCl (0.2 M) by vortex thoroughly for 0.5 min. After centrifugation at 16 000 × g for 5 min, 100 μl upper aqueous phase containing PYO was transferred to a 96-well plate and its absorbance was measured at 510 nm. Concentration of PYO was determined according to the standard curve.

RESULTS

A transferrable and integrative I-F Cascade is developed and is active in the recipient *P. aeruginosa* host

Our previous study has demonstrated that the type I-F CRISPR–Cas system encoded in the *P. aeruginosa* PA154197 strain is highly active for DNA interference and genome editing (13). Hence, we set out to construct a transferrable I-F Cascade for heterologous applications based on this system. The I-F Cascade encompasses Cas8f (Csy1), Cas5 (Csy2), Cas7 (Csy3) and Cas6 (Csy4) proteins which constitute the complex for CRISPR RNA (crRNA) biogenesis and DNA targeting and the Cas2-3 fusion protein for DNA degradation (Figure 1A) (39,40). To enable stable expression of a heterologous Cascade in recipient cells and to circumvent the dependence of antibiotics to maintain the system, we employ an integration-proficient vector containing a *lacZ* reporter, mini-CTX-*lacZ* (41), to deliver and integrate the I-F Cascade into the recipient genome. The vector carries an fCTX integrase gene *Int* and a single fCTX attachment site *attP* which enable the integration of the entire backbone into the highly conserved *attB* site in *P. aeruginosa* genomes *via* site-specific recombination (Figure 1B). The complete I-F *cas* operon with its native promoter (8.693 kb) which encodes all the *cas* genes, i.e. *cas1-cas2-3-cas8f-cas5-cas7-cas6*, was amplified from PA154197 genomic DNA and was cloned to the KpnI site in the mini-CTX-*lacZ* vector downstream of the FRT site for integration. To facilitate the screening of integration-positive clones, a strong housekeeping promoter P*tat* (42) is placed upstream of the promoter-less *lacZ* in the original mini-CTX-*lacZ* vector for blue/white colony selection, resulting in a 17.757-kb mini-CTX-IF-P*tat-lacZ* plasmid (termed as the transferrable I-F Cascade, pAY6924) (Figure 1B). Considering that genetic modifications in prokaryotes predominantly rely on the homology-directed repair (HDR) and most bacteria lack an efficient intrinsic homologous recombination system, we also developed an advanced transferrable I-F plasmid to simultaneously include an inducible phage λ-Red recombination system (AraC, P_{BAD}, Exo, Gam and Beta, 3.455 kb) at the SalI site downstream of the I-F *cas* operon, yielding a 21.212-kb transferrable plasmid mini-CTX-IF-λ_{red}-P*tat-lacZ* termed as the transferrable I-F-λ_{red} Cascade (pAY7136) (Figure 1C). Integration of these transferrable I-F Cascade systems should allow a *P. aeruginosa* host to temporarily acquire a 'native' I-F *cas* operon in its genome, enabling execution of the native CRISPR–Cas-based genome editing which is efficient and simple (Figure 1D and E) (12–14).

To examine the transferability and applicability of the system, we first delivered the transferrable I-F Cas-

cade (pAY6924) and the transferrable I-F-λ_{red} Cascade (pAY7136) into a CRISPR-free, model strain PAO1 by conjugation. All clones obtained displayed blue color (Figure 1F), suggesting the successful and efficient chromosomal integration of the cassettes. The resulting constructs were termed as PAO1^{IF} and PAO1$^{IF\lambda}$, respectively. A representative PAO1$^{IF\lambda}$ clone was subjected to whole genome sequencing (WGS) which revealed that the cassette was site-specifically integrated at the *attB* site (Genomic location: 2,947,580–2,947,610) (Figure 1G) and no undesirable genetic changes occurred except for a 4-bp synonymous substitution in the *ccoN1*_3 gene (Supplementary Table S2). RT-qPCR analysis showed that the integrated *cas* genes were all expressed in the transferred host PAO1^{IF} (Figure 1H). The integrated element did not cause alterations to the physiology of the host (Supplementary Figure S1). Whole genome transcriptome analysis and subsequent RT-qPCR quantification identified only one differentially expressed gene PA1137 which encodes a predicted oxidoreductase with the cut-off value of 2-fold higher in the transferred host PAO1^{IF} relative to the PAO1 WT. (Supplementary Figure S1B and C). These results demonstrated that the transferrable I-F Cascade is efficiently integrated and adequately expressed in the CRISPR-free host strain without perturbing the physiology of the recipient cells.

Next, we assessed the DNA interference activity of the transferred I-F Cascade by supplying a self-targeting plasmid (pAY7181) which expresses a crRNA targeting to a genomic locus *rhlI* gene (11). Delivery of the plasmid into PAO1^{IF} and PAO1$^{IF\lambda}$ by conjugation resulted in a conjugation recovery rate 6-magnitude lower (conjugation efficiency of 0.002% and 0.003%, respectively) than that of the control plasmid pAY5211 (Figure 1I), indicating that the transferred I-F Cascade displays a high DNA interference activity in the transferred hosts PAO1^{IF} and PAO1$^{IF\lambda}$, resulting in genome cleavage and cell death. The high DNA interference activity was maintained in the PAO1$^{IF\lambda}$ host after 20 generations of growth in the absence of antibiotic selection (Figure 1I), demonstrating the stable integration and function of the transferred I-F Cascade in the recipient strain.

Transferrable type I-F system displays a substantially greater DNA interference capacity than the transferrable Cas9 system

We next compared the DNA interference activity of the transferrable type I-F Cascade we developed with a transferrable Cas9 system. A similar transferrable Cas9 system (pAY7166) was firstly constructed by replacing the I-F Cascade and its promoter in the mini-CTX-IF-λ_{red}-P*tat*-*lacZ* vector (pAY7136) with the Sp*cas9* gene driven by a P_{BAD} promoter (Supplementary Figure S2A). Integration of pAY7166 into PAO1 generated a PAO1 variant integrated with the Sp*cas9* and λ-Red genes at the *attB* site, termed as PAO1$^{Cas9\lambda}$. The expression of *cas9* and λ-Red genes in this strain was confirmed by RT-qPCR analysis (Supplementary Figure S2B). Considering that the type I-F Cascade recognizes a PAM sequence of 5′-CC-3′ located at the 5′-end of a 32-bp protospacer and the Cas9 effector recognizes a PAM sequence of 5′-NGG-3′ located at the 3′-end of a 20-bp protospacer (43), to compare the DNA interference activity of the transferred I-F and Cas9 systems, we designed pairs of crRNAs expressed from the self-targeting plasmids (pTargeting) such that they are recognized by the two effectors, respectively, and target to protospacers sharing maximal overlap (Figure 2A). Three pairs of protospacers were targeted and they are located in the integrated DNA region, including one pair in the P*tat* promoter (IF_Ps1/Cas9_Ps1) and two pairs in the *lacZ* coding region (IF_Ps2/ Cas9_Ps2 and IF_Ps3/Cas9_Ps3) (Figure 2A). Following delivery of each of the targeting plasmids into PAO1$^{IF\lambda}$ or PAO1$^{Cas9\lambda}$ by conjugation, the numbers of recovered colonies relative to that of the corresponding control plasmid which does not express the programmed self-targeting mini-CRISPR were recorded to indicate the DNA interference activity of the two effectors. The transferred I-F Cascade effected a strong self-targeting activity toward all three selected protospacers as evidenced by a 6-magnitude reduction of colony recovery relative to that of the control plasmid, i.e. conjugation efficiency of 0.0007% (IF_Ps1), 0.0003% (IF_Ps2), and 0.0001% (IF_Ps3) (Figure 2C), respectively. However, the transferred Cas9 system only effected 1-magnitude reduction of colony recovery upon introduction of the three pTargeting plasmids relative to the conjugation of the control plasmid, i.e. conjugation efficiency of 25.2% (Cas9_Ps1), 45.6% (Cas9_Ps2) and 52.0% (Cas9_Ps3), respectively (Figure 2D), indicating that the transferred I-F Cascade displays a substantially greater targeting capacity than the transferred Cas9 system.

To exclude the possibility that the poor targeting activity of the transferred Cas9 was due to the locations of the protospacers selected, we examined the targeting of the two effectors to four additional pairs of protospacers located in the opposite strands and in an endogenous gene locus *rhlI*. The four pairs of corresponding spacer sequences employed share an identical PAM location distributed in the complementary strand of the protospacer and display 20-bp complementarity (Figure 2B). Following introduction of the corresponding pTargeting into PAO1$^{IF\lambda}$ and PAO1$^{Cas9\lambda}$, the transferred I-F system displayed a substantially higher targeting capacity to all these four sites than the transferred Cas9 system, as evidenced by the conjugation efficiency of 0.0002% (IF_Ps4), 0.0001% (IF_Ps5), 0.0002% (IF_Ps6) and 0.0016% (IF_Ps7) as opposed to 55.7% (Cas9_Ps4), 45.9% (Cas9_Ps5),42.9% (Cas9_Ps6) and 69.6% (Cas9_Ps7) effected by the Cas9 system (Figure 2E and F), further demonstrating the substantially higher targeting capacity of the transferred I-F system than the Cas9 system in *P. aeruginosa*.

Activity of the transferrable I-F Cascade was further compared with a plasmid-borne Cas9 which was developed and employed by Chen *et al* in a modified two-plasmid-based genome-editing system (25). A pair of pTargeting that targets to the protospacer IF_Ps7 and Cas9_Ps7 located in the *rhlI* gene was employed (Figure 2B). The transferred I-F Cascade was found to display a comparable DNA interference activity with this plasmid-borne Cas9 as demonstrated by the similar conjugation efficiencies (0.001–0.002%) effected by the two effectors (Figure 2G and H). However, when these two systems were assessed in several additional *P. aeruginosa* strains such as PA14 and two clinical iso-

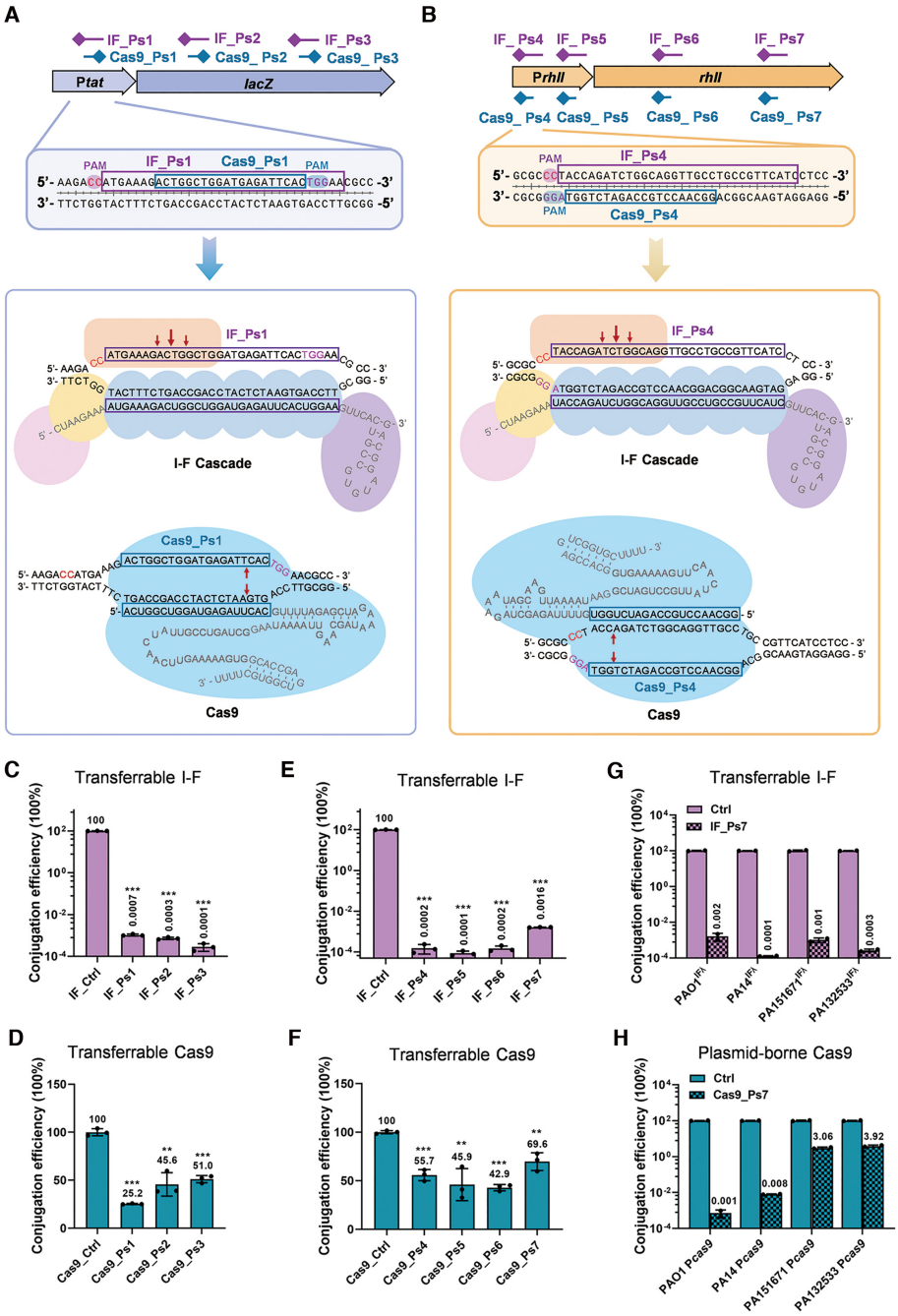

Figure 2. The transferrable I-F Cascade displays a substantially greater targeting capacity than the transferrable and the plasmid-borne Cas9 systems. (**A, B**) Schematic diagram of the DNA interference assay. Pairs of the targeting sites (protospacers) located in both the integrated region P*tat-lacZ* (A) and the endogenous region P*rhlI-rhlI* (B) were employed to compare the DNA interference activity of the transferred type I-F Cascade and the transferred Cas9 in PAO1$^{IF\lambda}$ and PAO1$^{Cas9\lambda}$ cells, respectively. Each pair of the protospacers contains one applied for the I-F Cascade and one for Cas9 with following features: three pairs (IF_Ps1/Cas9_Ps1, IF_Ps2/Cas9_Ps2 and IF_Ps3/Cas9_Ps3) are located in the same DNA strand with maximal overlap in each pair (A); four pairs (IF_Ps4/Cas9_Ps4, IF_Ps5/Cas9_Ps5, IF_Ps6/Cas9_Ps6 and IF_Ps7/Cas9_Ps7) are located in the complementary strands and share the same PAM location (B). Diamonds denote the PAM sequences. The nucleotide sequences of the protospacer pair IF_Ps1/Cas9_Ps1 (A) and IF_Ps4/Cas9_Ps4 (B) and the resulting targeting pattens mediated by the I-F Cascade and Cas9 are shown in the lower panels. The 32-bp protospacer for the I-F Cascade targeting is framed in purple boxes and the 20-bp protospacer for Cas9 targeting is framed in blue boxes. (**C**, **D**) DNA interference activity of the transferred I-F Cascade (C) or the transferred Cas9 effector (D) determined by the colony recovery rate of pTargeting transformation relative to control plasmid (lacking the mini-CRISPR array) transformation via conjugation, i.e. conjugation efficiency. The protospacer site targeted by the employed pTargeting is shown (x-axis). A low conjugation efficiency indicates a high DNA interference activity exhibited by the effector examined. (**E**, **F**) DNA interference activity of the transferred I-F Cascade (E) or the transferred Cas9 (F) determined by the conjugation efficiency of indicated pTargeting transformation. pTargeting is denoted by the corresponding protospacer site (x-axis) it targets to. (**G, H**) DNA interference activity of the transferred I-F Cascade (G) or the plasmid-borne Cas9 (H) determined by the conjugation efficiency of transforming the pTargeting plasmids that target to the IF_Ps7 (G) or Cas9_Ps7 (H) site, respectively, into the indicated host strains PAO1, PA14, PA151671 and PA132533 (x-axis). Data are the mean of three (B, C, D, F) or two (G, H) biological repeats and are expressed as mean ± SD. Statistical significance is calculated based on Student's *t* test (*$P < 0.05$; **$P < 0.01$; ***$P < 0.001$).

lates PA151671 and PA132533 (Supplementary Figure S3), we found that the transferrable I-F Cascade displayed a greater targeting capacity than the plasmid-borne Cas9 as demonstrated by the conjugation efficiency of the pTargeting (IF_Ps7) as 0.0001%, 0.001% and 0.0003%, respectively, in PA14$^{IF\lambda}$, PA151671$^{IF\lambda}$ and PA132533$^{IF\lambda}$, whereas that of the corresponding pTargeting (Cas9_IF7) effected by the plasmid-borne Cas9 system were 0.008%, 3.06% and 3.92%, respectively (Figure 2G and H). These results demonstrated that the transferrable I-F Cascade system exhibits substantially greater DNA interference capacity, efficiency, and strain stability than both the transferrable and plasmid-borne Cas9-based systems, underscoring its application potentials for widespread heterologous genome editing.

The transferred I-F Cascade is reprogrammable for various genetic exploitations in the model heterologous host PAO1

We next examined the applicability of the transferred I-F Cascade in PAO1^{IF} for genome editing using deleting *rhlI* gene as an example which has been shown to display a readily detectable phenotype, i.e. loss of the green-blue pigmented pyocyanin (PYO) production compared with the WT (44). We employed the strategy established for the native I-F Cascade meditated genome editing which is achieved by one-step transformation of a single editing plasmid (13). An editing plasmid termed as p*rhlI*-Del-1 (pAY7420) was constructed by assembling ∼800-bp upstream and ∼800-bp downstream homologous arms of *rhlI* into the *rhlI*-targeting plasmid pAY7181 employed in the self-targeting assay for HR-mediated *rhlI* deletion (Figure 3A and Supplementary Figure S4A) (28). The editing plasmid also encodes a *lux* operon in its backbone (13), enabling luminescence-based screening for the desired colonies following introduction of p*rhlI*-Del-1 into PAO1^{IF} by conjugation. Ten clones displaying high luminescence intensity were analyzed by colony PCR and all clones were shown to harbor the desired *rhlI* deletion (Supplementary Figure S4B and Figure 3B), demonstrating the applicability and high efficiency of the transferred type I-F Cascade for genome editing in the recipient host. To evaluate the editing efficiency in a larger population of recovered clones, we examined 48 luminescence-positive clones by colony PCR which showed that 37 clones harbored the desired *rhlI* deletion (Supplementary Figure S4C). Abolishment of the green-blue pigmented PYO was also observed in all 37 clones compared to the WT PAO1 (Supplementary Figure S4D). Based on two rounds of independently conducted editing reactions, an average efficiency of 81.3% was obtained (Figure 3C).

We also examined the editing capacity of the transferred I-F Cascade mediated by a less effective crRNA, i.e. that targets to the protospacer sequence IF_Ps7 (conjugation efficiency of 0.0016% vs. 0.0002% for IF_Ps6). Delivery of the corresponding editing plasmid p*rhlI*-Del-2 into PAO1^{IF} by conjugation resulted in 33.3% editing efficiency (Figure 3C), indicating that the loci structure of the selected targeting site (protospacer) affects editing efficiency. Editing capacity of the transferred I-F Cascade by employing a tandem mini-CRISPR cassette (p*rhlI*-Del-3) which simultaneously targets to the IF_Ps6 and IF_Ps7 protospacers (Supplementary Figure S4A) was determined to be 77.1% (Figure 3C), suggesting simultaneously targeting to multiple protospacers represents an effective strategy to circumvent the poor targeting effected by an inefficient protospacer site.

We next examined the site specificity of the transferred I-F Cascade-mediated genome editing and the possible causes of false positive clones. Three clones which have been verified to harbor Δ*rhlI* and three false positive clones which displayed luminescence but was shown to contain an intact *rhlI* allele were subjected to WGS analysis. Precise *rhlI* deletion without off-target mutation was verified in all three authentic Δ*rhlI* clones (Figure 3D), demonstrating that the type I-F Cascade-mediated genome editing is highly site-specific. Interestingly, in all three false positive clones, mutations in the *cas* genes were identified, i.e. 33-bp deletion in *cas2-3* in one clone and point mutations in *cas5* in two clones (Supplementary Table S2), which cause inactivation of the nuclease Cas2-3 and premature termination of Cas5, respectively. These results suggested that mutations in *cas* genes represent a major reason for the emergence of false positive clones which is consistent with several previous studies about CRISPR-based genome editing (45–47).

To test the robustness of the transferred I-F Cascade to construct other types of genetic editing, gene (or DNA fragment) insertion such as N-terminal *FLAG*-tagging of *mexF* gene and C-terminal *gfp*-tagging of *rhlA* gene, and a C54T point mutation in *rhlI* were carried out (Supplementary Figure S5A and B). Randomly screening ten luminescence-positive clones recovered from conjugation of the corresponding editing plasmid into PAO^{IF} resulted in 7/10, 5/10 and 1/10 desired clones for N-terminal *FLAG*-tagging of *mexF*, *gfp*-tagging to the C-terminal of *rhlA*, and the C54T point mutation in *rhlI*, respectively (Supplementary Figure S5C and D), confirming the robustness of the transferred I-F Cascade for genetic manipulations.

An advanced transferrable I-F-λ_{red} system enables genome editing in genotypes with a poor intrinsic homologous recombination capacity

We next expand the application of the transferrable I-F Cascade to PA14, a strain with an existing native type I-F CRISPR–Cas system in its genome. We first compared the DNA interference activity effected by the native I-F Cascade in PA14 and that in combination with an additional Cascade from PA154197 integrated at the *attB* site in the PA14^{IF} strain. Introduction of a self-targeting plasmid pAY7138 (targeting to the protospacer IF_Ps1) resulted in a conjugation efficiency of 6-magnitude lower relative to the control plasmid pAY5211 in both strains (Figure 3E), indicating the strong DNA interference activity of the native I-F system in PA14 and that presence of an additional I-F Cascade did not further enhance the DNA interference activity in the resulting cells. Surprisingly, when the editing plasmid p*rhlI*-Del-3 was delivered into the two cells, PA14 and PA14^{IF}, to construct *rhlI* gene deletion, a very low editing efficiency (11.5% and 15.6%) was obtained in both cells (Figure 3F), indicating that the intrinsic homologous recombination capacity in PA14 is poor and is not sufficient to repair the DNA breakage occurred in the self-targeting step. Indeed, employing a genetic assay described by Rodríguez-

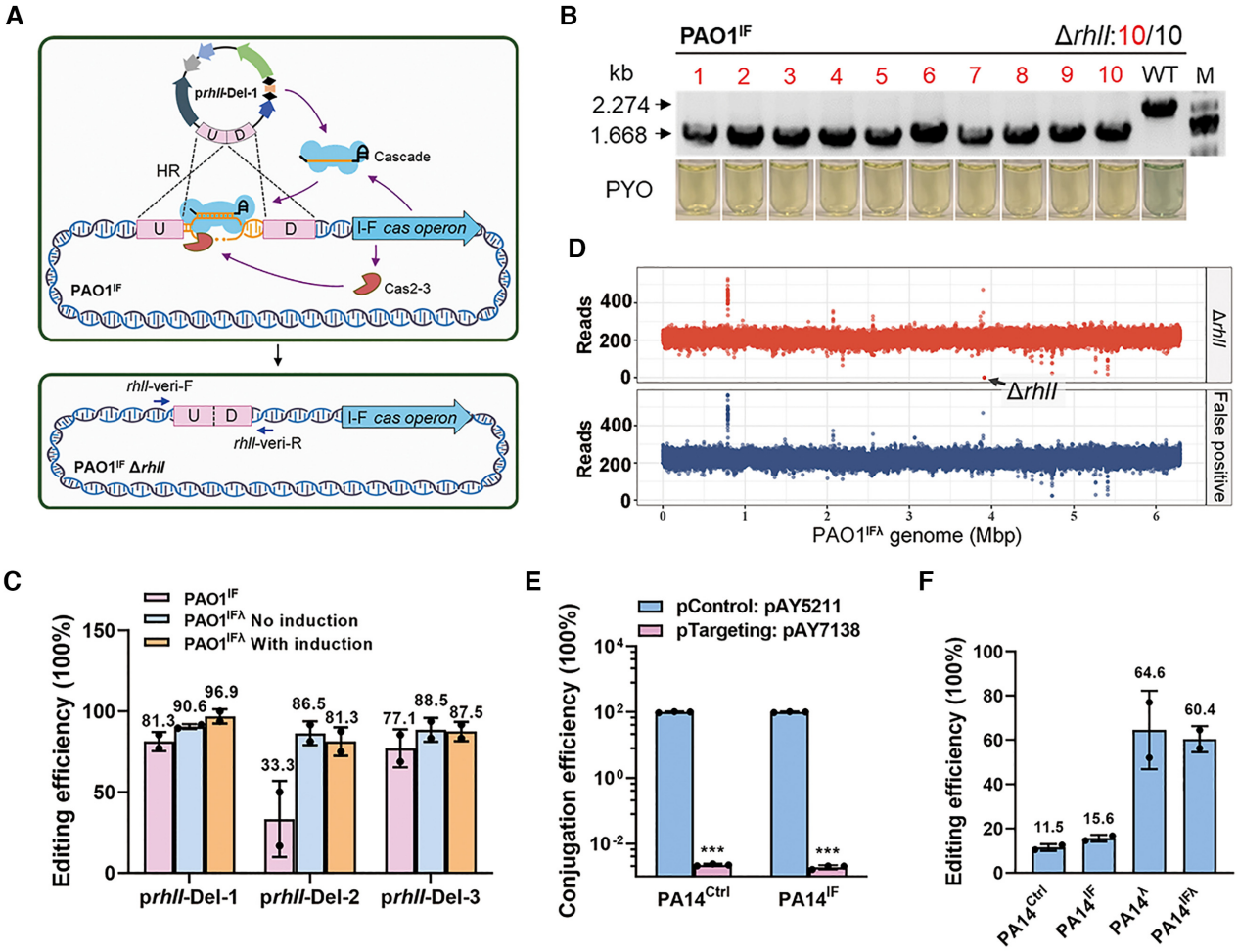

Figure 3. Transferred I-F Cascade-mediated precise and efficient gene deletion in PAO1 and PA14. (**A**) Schematic diagram of the transferred I-F Cascade-mediated genome editing by one-step transformation of a single editing plasmid p*rhlI*-Del-1. The editing plasmid expresses a *rhlI*-targeting crRNA and provides a donor template which consists of 833-bp upstream (U) and 805-bp downstream (D) homologous arms of the *rhlI* gene for homologous recombination (HR)-mediated repair. Cascade targeting recruits Cas2-3 to generate DNA breakage within the *rhlI* gene. HR between the donor and its homologous arms flanking the *rhlI* gene results in the desired *rhlI*-deletion mutant. (**B**) Verification of the precise *rhlI* deletion in the PAO1^{IF} host by colony PCR. Primer pairs used to verify *rhlI* deletion in this study are indicated in (a). Clone numbers with desired *rhlI* deletion are highlighted in red. Production (WT) or loss (mutant) of the blue-green colored pigment PYO in the corresponding inoculum is shown in the lower panel. M: Marker. (**C**) Editing efficiency of the transferred I-F (PAO1^{IF}) or I-F-λ_{red} (PAO1$^{IF\lambda}$) system employing the indicated editing plasmids (x-axis) with or without L-arabinose induction. (**D**) Representative mapped WGS reads of the authentic Δ*rhlI* mutant (red) and false positive clone (blue) against the PAO1$^{IF\lambda}$ genome. Arrow indicates the absence of reads at the *rhlI* locus in the Δ*rhlI* clone. (**E**) DNA interference activity of the native (PA14^{Ctrl}) and transferred (PA14^{IF}) I-F Cascades determined by the conjugation efficiency of transforming pAY7138 that targets to IF_Ps1 (Figure 2A). (**F**) Editing efficiency of the native and transferred I-F Cascade systems in the indicated host strains. PA14^{Ctrl}: PA14 strain integrated with the empty transferrable system lacking the *cas* operon; PA14^{IF}: PA14 strain integrated with the transferrable I-F Cascade; PA14$^{\lambda}$: PA14 strain integrated with the transferrable system carrying the λ-Red recombination system; PA14$^{IF\lambda}$: PA14 strain integrated with the transferrable I-F-λ_{red} Cascade. Data are the mean of two (C and H) or three (G) biological repeats and are expressed as mean ± SD. Statistical significance is calculated based on Student's *t* test (***$P < 0.001$).

Beltrán et al (48), the intrinsic recombineering efficiency in PA14 is quantified to be only 29% relative to that of PAO1 (Supplementary Figure S6).

To overcome this impediment, we employed the advanced I-F-λ_{red} cassette (pAY7136) we developed which contains both the PA154197 I-F Cascade and a λ-Red recombination system driven by the P_{BAD} promoter to construct *rhlI* deletion in PA14. Upon induction of the λ-Red system with 20 mM L-arabinose which is sufficient to induce the expression of λ-Red genes to high level (Supplementary Figure S5E), an editing efficiency of 60.4% was achieved for constructing Δ*rhlI* employing the editing plasmid p*rhlI*-Del-3 (Figure 3F), which is 4-fold higher than that achieved in the PA14^{IF} host (15.6%). This result demonstrated the advantage of the transferrable I-F-λ_{red} cassette which enables the I-F Cascade-mediated genome editing in a recombination-poor genotype. The advantage of the transferrable I-F-λ_{red} system was also demonstrated in the PAO1 background as evidenced by an increase of editing efficiency from 33.3% to >80% for constructing Δ*rhlI* in the PAO1$^{IF\lambda}$ host relative to the PAO1^{IF} host employing the same editing plasmid p*rhlI*-Del-2 (Figure 3C), suggesting that a greater homologous recombination capacity can also improve the editing efficiency by compensating for the inefficient targeting of a

programmed crRNA. Interestingly, we found that in PAO1 background, basal or leaky expression (Supplementary Figure S5F) of the λ-Red system without L-arabinose induction is sufficient to improve the editing efficiency (Figure 3C).

The transferrable I-F Cascade is readily applied in diverse *P. aeruginosa* genetic backgrounds and other *Pseudomonas* species

To examine the widespread application of the transferrable I-F-λ_{red} system, we integrated the I-F-λ_{red} cassette into three clinical *P. aeruginosa* isolates with diverse genetic backgrounds and virulence capacities (Supplementary Table S3 and Figure S3): PA150577, PA132533, PA151671, and characterized the DNA interference activity and editing exploitations of the system in the resulting cells. Among the three strains, the genome sequence of PA150577 is available. Hence, a CRISPRCasFinder (49) analysis was firstly conducted to examine whether the strain contains native CRISPR–Cas systems. A complete native type I-F CRISPR–Cas loci was identified in this strain which is organized in a sandwich structure of CRISPR1-Cas-CRISPR2 and shares 98.69% identity with that in PA154197 (Supplementary Figure S7A). However, DNA interference activity of this native CRISPR–Cas system was found to be poor as evidenced by only 2-magnitude reduction of colony recovery upon introduction of the targeting plasmid pAY7138 relative to the control plasmid (Figure 4A), as opposed to 5- to 6-magnitude reduction necessary to achieve genome editing as described above. PA132533 and PA151671 are clinical isolates without available genome information. We then conducted PCR analysis to identify the presence of native I-F CRISPR–Cas systems in these genomes. Presence of all six I-F Cascade genes was shown in PA151671 (Supplementary Figure S7B). However, introduction of the targeting plasmid pAY7138 did not reveal any DNA interference activity in the cell, indicating that the native type I-F system in PA151671 is inactive (Supplementary Figure S7C). In PA132533, PCR analysis indicated that the strain contains an incomplete I-F Cascade which lacks the *cas8f* gene (Supplementary Figure S7B).

We then transferred the I-F-λ_{red} cassette into these three strains. Stable integration and expression of the cassette was confirmed by the blue colonies on the X-gal plate and RT-qPCR analysis (Supplementary Figure S8). Sufficiently high DNA interference activities were detected in all three resulting strains PA150577$^{IF\lambda}$, PA132533$^{IF\lambda}$ and PA151671$^{IF\lambda}$ (Figure 4A). Genome editing in the resulting cells was conducted by directly introducing the editing plasmid p*rhlI*-Del-3. A successful rate of 2/10, 4/10 and 3/10 was achieved in one-step, single conjugation reaction in the PA150577$^{IF\lambda}$, PA132533$^{IF\lambda}$ and PA151671$^{IF\lambda}$ cells, respectively (Figure 4B), demonstrating the robust editing capacity of the transferred I-F Cascade in diverse *P. aeruginosa* genotypes.

Next, we examined the applicability of the transferrable I-F system in other *Pseudomonas* species, such as *P. putida* which is endowed with many traits desired for bioproduction and bioremediation. The I-F-λ_{red} cassette was readily integrated into the *P. putida* KT2440 genome. We then conducted editing using deleting the *algR* gene as an example in the resulting cells by one-step introduction of the editing plasmid pAYKT2440 *via* conjugation. A 10/10 (100%) editing efficiency was obtained (Figure 4B), demonstrating the applicability of the transferrable I-F system in other *Pseudomonas* species. Similar to the observation in PAO1 background, the basal or leaky expression of the λ-Red system was found to be sufficient for genome editing in *P. putida* KT2440. Together, these results demonstrated the powerful editing capacity of the transferrable I-F-λ_{red} system we developed which effected editing in diverse *P. aeruginosa* genetic backgrounds with and without native CRISPR–Cas systems, with and without available genome sequences, and in other *Pseudomonas* species such as *P. putida.*

Application of the transferrable and integrative I-F Cascade in the *acr*-containing strains

Anti-CRISPR (Acr) is a common mechanism that inhibits the CRISPR–Cas immunity (50,51). More than 30% of sequenced *P. aeruginosa* genomes were found to carry one or more *acr* genes (20). We examined four additional *P. aeruginosa* strains, including two clinical isolates ATCC 27853 (termed as PA27853 herein) and PA130788 and two environmental strains PA238 and PA1155 in which presence of *acr* genes were indicated by the Acr prediction program AcrFinder (52) (Supplementary Figure S9A). The I-F-λ_{red} cassette was readily integrated into the *attB* site of the four genomes and were stably expressed as shown by RT-qPCR analysis (Supplementary Figure S8). However, no DNA interference activity was detected in PA13088, PA238, PA1155, confirming the presence of Acrs (Note that DNA interference activity cannot be examined by the pTargeting we designed in PA27853 owing to its intrinsic kanamycin resistance) (Supplementary Figure S9B). We next used PA130788 as a model to examine whether deleting *acr* genes will activate the transferred I-F Cascade and enable genome editing in these genotypes. We deleted the *acr* gene together with its associated gene *aca* in PA130788 (Figure 4C) using the counter selection-based method (53), generating a mutant PA130788 Δ*acr-aca*. As shown in Figure 4A, the transferred I-F-λ_{red} Cascade in this mutant was activated to execute self-targeting DNA breakage as evidenced by a 5-magnitude reduction of the colony recovery rate upon introduction of the pTargeting plasmid pAY7138 relative to the control plasmid pAY5211, confirming that the failure of self-targeting in PA130788$^{IF\lambda}$ was indeed caused by the identified Acr. Construction of Δ*rhlI* by introducing the single editing plasmid p*rhlI*-Del-3 in PA130788 Δ*acr-aca* achieved 10/10 editing efficiency (Figure 4B). These results demonstrated the applicability of the transferred I-F-λ_{red} system in *acr*-containing strains upon removal this element by an alternative approach.

Repurposing the transferred I-F Cascade for transcriptional modulation

In addition to anti-CRISPR elements, inability to transfer plasmids due to poor DNA uptake capacity or the lack of suitable replicating vector in certain genotypes also impedes genome editing (11). Multidrug resistance in clini-

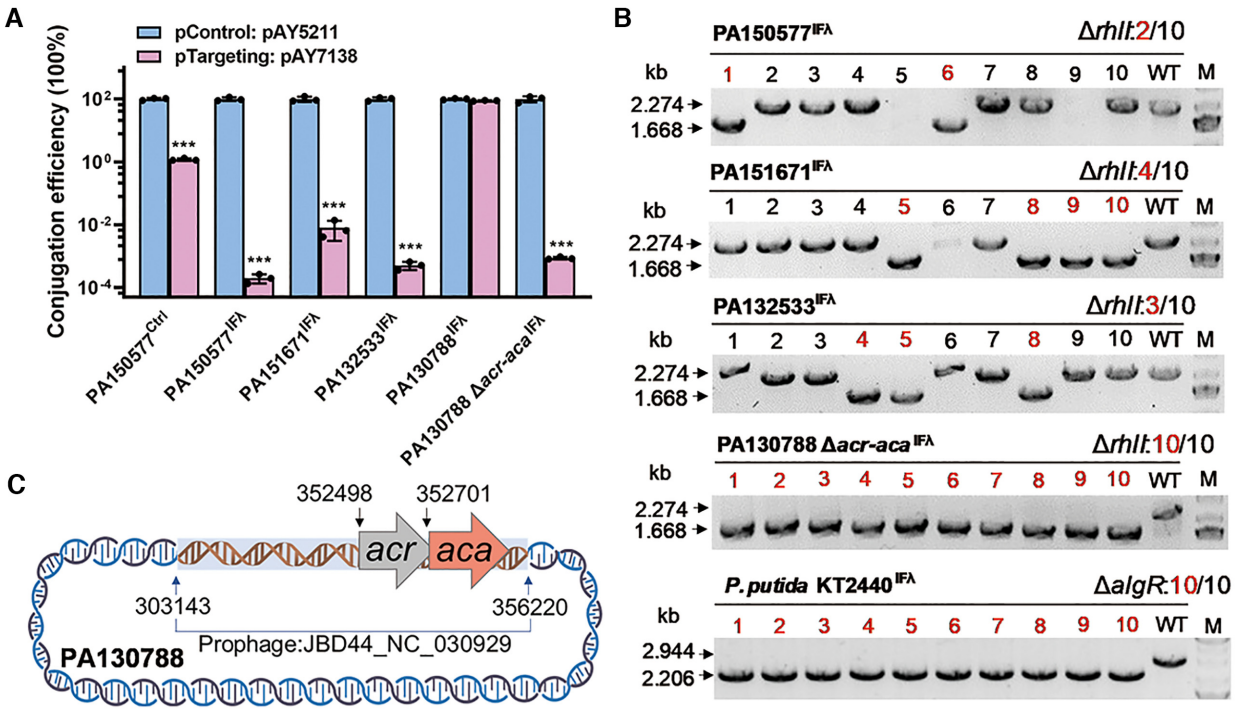

Figure 4. Transferrable I-F-λ_{red} Cascade enables gene deletion in diverse *Pseudomonas* genetic backgrounds. (**A**) DNA interference activity of the transferred I-F Cascade determined by the conjugation efficiency of transforming pAY7138 (targeting to the IF_Ps1 protospacer site) into the indicated host strains PA150577^{ctrl}, PA150577$^{IF\lambda}$, PA151671$^{IF\lambda}$, PA132533$^{IF\lambda}$, PA130788$^{IF\lambda}$, and PA130788 Δ*acr-aca*$^{IF\lambda}$ (x-axis). (**B**) Verification of the precise *rhlI* deletion in the indicated host strains PA150577$^{IF\lambda}$, PA151671$^{IF\lambda}$, PA132533$^{IF\lambda}$, PA130788 Δ*acr-aca*$^{IF\lambda}$ and *algR* deletion in *P. putida* KT2440$^{IF\lambda}$ by colony PCR. Primer pairs used to verify *rhlI* deletion in this study are indicated in Figure 3A. Clone numbers with desired gene deletion are highlighted in red. (**C**) Schematic diagram of an anti-CRISPR gene *acr* and its associated repressor gene *aca* located in the prophage JBD44_NC_030929 region in PA130788. Data are the mean of three biological repeats and are expressed as mean ± SD. Statistical significance is calculated based on Student's *t* test (***$P < 0.001$).

cal strains poses another barrier for delivery of the editing plasmid and selection of transformants. PA27853 represents such a genotype in which the CRISPR–Cas-based genome editing is hindered by both Acrs and its intrinsic resistance to kanamycin which restrained the transformation and selection of the series of targeting and editing plasmids we developed. To overcome these impediments, we set out to develop an 'all-in-one' transferrable I-F Cascade-based transcriptional interference system mini-CTX-CRISPRi-*lacZ* (transferrable CRISPRi) for transcriptional modulation without the requirement of delivering an editing plasmid. The transferrable I-F Cascade-based CRISPRi system (pAY6925) was constructed by removal of the *cas*2-3 gene in the transferrable I-F Cascade (pAY6924) to disable its DNA cleavage ability (Figure 5A). It is expected that with the provision of a programmed crRNA, the Cascade complex is able to recognize and bind to the complement genomic locus specifically, resulting in transcriptional repression by preventing the recruitment of RNA polymerase (RNAP) and blocking the transcription of the target gene (Figure 5B) (54). To bypass the delivery of additional plasmids such as that expressing a programmed crRNA for desired genomic site targeting, we designed a multi-cloning site downstream of the P*tat* promoter in the mini-CTX-CRISPRi-*lacZ* backbone such that a mini-CRISPR fragment can be readily assembled into the integrative cassette and be delivered into the strains of interest along with the I-F CRISPRi element. Upon stable integration of the cassette in the host genome, the crRNA will be constitutively expressed from the P*tat* promoter, eliciting robust Cascade binding to the target site and transcription repression (Figure 5A).

We first tested the applicability of the transferrable I-F Cascade-based CRISPRi system in the model strain PAO1. We constructed five transferrable mini-CTX-CRISPRi-*rhlI* plasmids, each expressing a crRNA targeting to a distinctive location in the *rhlI* gene or its promoter region (Figure 5C), including a region bound by the RNAP (Ps-1, –152 ~ –120 bp), the transcription initiation region (Ps-2, –63 ~ –31 bp), the 5′-end of the *rhlI* coding region (Ps-3, 54 ~ 86 bp), the middle region of the *rhlI* gene (Ps-4, 238 ~ 270 bp), and the 3′-end of the *rhlI* coding region (Ps-5, 520 ~ 552 bp). We assembled each of the five mini-CRISPRs into the transferrable I-F Cascade CRISPRi backbone, respectively, resulting in five CRISPRi constructs, mini-CTX-CRISPRi-*rhlI*-1 to 5. Introduction of each of these plasmids in PAO1 resulted in simultaneous integration of the I-F CRISPRi Cascade and a mini-CRISPR array expressing a *rhlI*-targeting crRNA at the *attB* site of PAO1. Three clones of each of the resulting constructs were selected to quantify the *rhlI* transcriptional levels. Among them, the construct integrated with the mini-CRISPR-2 and mini-CRISPR-3 displayed significant (51% and 71% reduction, respectively) repression of *rhlI* expression (Figure 5D). crRNAs expressed from these two mini-CRISPRs target to the regions located at the transcription initiation site (Ps-2)

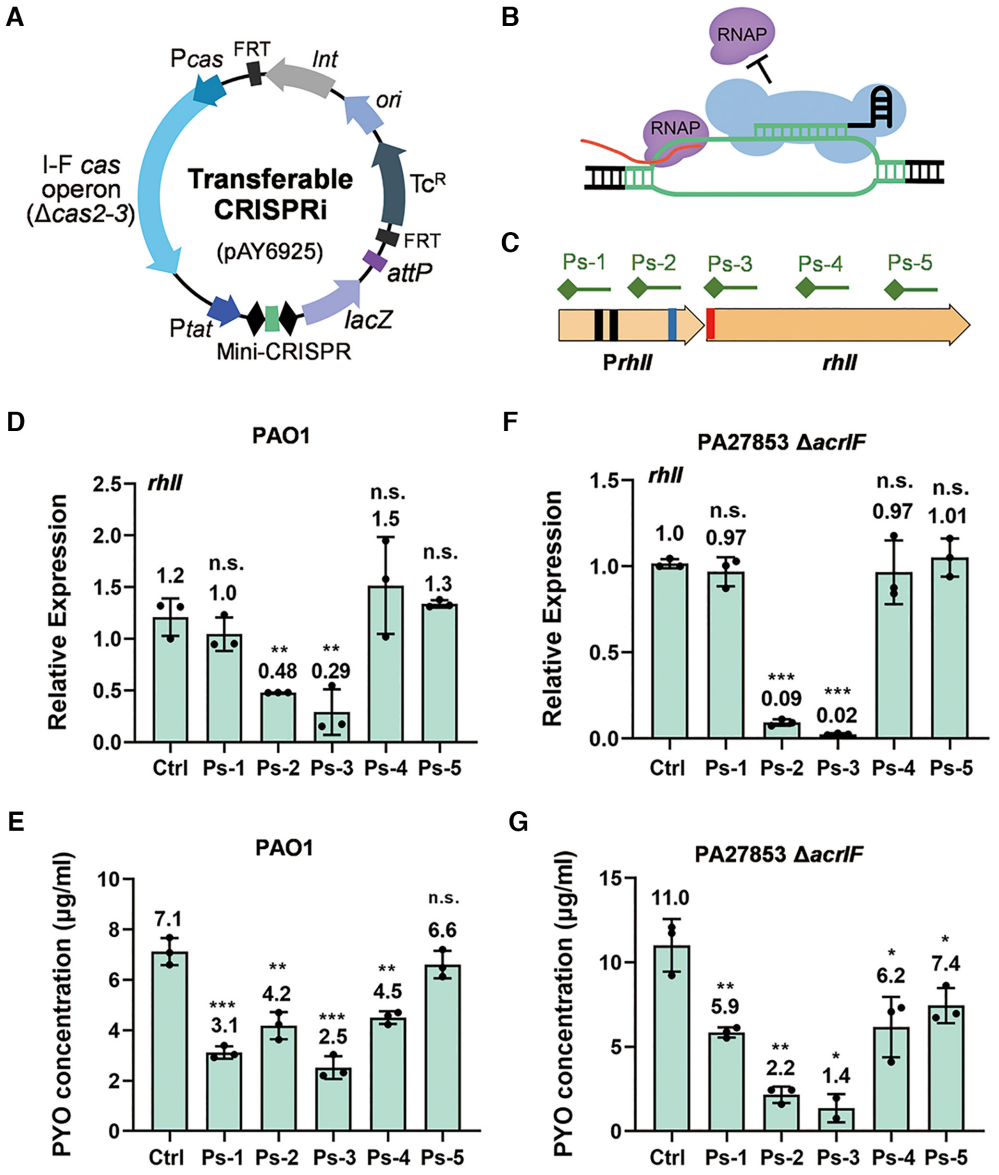

Figure 5. Transferrable I-F CRISPRi-mediated gene repression. (**A**) Diagram of the elements and organization of the transferrable I-F CRISPRi system. A truncated *cas* operon lacking the *cas2-3* gene replaced the complete *cas* operon as in the transferrable I-F Cascade (pAY6924). A programmed mini-CRISPR is assembled downstream of the P*tat* promoter. (**B**) Schematic diagram showing the working mechanism of the CRISPRi-based gene repression. Site-specific binding of the Cascade to a genomic locus prevents the recruitment of the RNA polymerase (RNAP) or blocks its operation in gene transcription. (**C**) Schematic diagram of the protospacers selected to examine the gene repression activity of the transferred CRISPRi system. Five protospacers located at different locations in the coding region of *rhlI* and its promoter region are selected. Diamonds denote the PAM sequences. Ps-1: –152 ∼ –120 bp; Ps-2: –63 ∼ –31 bp; Ps-3: 54 ∼ 86 bp; Ps-4: 238 ∼ 270 bp; Ps-5: 520 ∼ 552 bp. (**D, E**) Relative expression of *rhlI* (D) and PYO production level (E) in PAO1 cells transferred with a I-F CRISPRi targeting to the indicated sites (x-axis). (**F, G**) Relative expression of *rhlI* (F) and PYO production level (G) in PA27853 Δ*acrIF* cells transferred with a I-F CRISPRi targeting to the indicated sites (x-axis). Data are the mean of three biological repeats and are expressed as mean ± SD. Statistical significance is calculated based on Student's *t* test (n.s., not significant; **P* < 0.05; ***P* < 0.01; ****P* < 0.001).

and the 5′-end of the *rhlI* coding region (Ps-3). PYO levels in these cells are consistent with the corresponding *rhlI* gene repression (Figure 5E). No repression effect was observed by targeting to Ps-1, Ps-4 and Ps-5. Interestingly, although RT-qPCR showed no significant change on *rhlI* expression by targeting to Ps-1 and Ps-4, PYO level was reduced moderately in the cell, suggesting certain degree of repression. These results demonstrated the feasibility of the designed CRISPRi system for gene repression by one-step transfer and integration of the I-F CRISPRi Cascade together with a programmed mini-CRISPR. It also suggested that most effective repression requires the Cascade targeting at the transcription initiation site or its proximal region.

We next tested the applicability of the system in PA27853. To this end, the *acr* gene in PA27853 was firstly deleted using the two-step counter-selection method (53). Each of the five transferrable mini-CTX-CRISPRi-*rhlI* plasmids was delivered into PA27853 Δ*acrIF* by conjugation. RT-qPCR and

PYO production verified significant repression of *rhlI* effected by the cassette containing mini-CRISPR-2 and mini-CRISPR-3 (Figure 5F and G), consistent with the results obtained in PAO1 background. This result demonstrated that the transferrable and integrative I-F CRISPRi system we developed provides as a powerful and an alternative gene knockdown strategy for functional genomics without the need of plasmid transformation. The robustness of this system was further demonstrated in the strain PA154197 Δ*cas2-3* and an additional clinical isolate PA153301 which genome sequence is not available but was verified to be free of a complete endogenous type I-F CRISPR–Cas system, i.e. only the presence of *cas6* gene was detected (Supplementary Figure S7B). In both strains, one-step transformation and integration of the mini-CTX-CRISPRi-*rhlI* containing mini-CRISPR-2 and -3 resulted in repression of *rhlI* (Supplementary Figure S10).

We further compared the gene repression efficiency between the integrative and a plasmid-based CRISPRi systems which differ in copy numbers of the crRNA-expressing cassette (Supplementary Figure S11A). We constructed and introduced five targeting plasmids that encode crRNAs targeting to Ps-1-5 (Figure 5C), respectively, into the PA154197 Δ*cas2-3* strain to examine their effects on the *rhlI* expression. However, requirement of antibiotic to maintain the plasmids resulted in cell lysis at the stationary phase. Although significantly decreased PYO production was observed when Ps-2 and Ps-3 was targeted, respectively (Supplementary Figure S11B), cell lysis impeded the next step of transcriptional analysis. These results further highlighted the advantages of employing the chromosomal integrative CRISPRi system for transcriptional analysis.

Transferred I-F Cascade-mediated removal of the large integrated I-F-λ_{red} cassette

To generate clean gene deletion in the genetic background of interest, it is necessary to remove the transferred I-F Cascade. Although the mini-CTX-*lacZ* backbone was equipped with two FRT sites for removing the auxiliary elements in the vector such as the integrase gene *Int* and the tetracycline-resistant marker employing the ectopically expressed flippase (41), the I-F Cascade and the *lacZ* reporter remains at the *attB* site. To completely remove the integrated fragment following the desired genetic exploitations, we harnessed the processive degradation capacity of the Cas3 nuclease in the transferred I-F Cascade to delete the large-scale fragment of I-F-λ_{red} Cascade (21.212 kb). The *lacZ* reporter included in the fragment serves as an indicator for successful removal of the whole cassette with a desired white colony phenotype on the X-gal plate. A 22.298-kb Cascade-removal plasmid pAY7401 (Figure 6A) was constructed by assembling a crRNA targeting to the *lacZ* gene and a donor sequence consisting of ∼5-kb upstream and ∼5-kb downstream homologous arms of the *attB* site. We tested the capacity of this editing plasmid in the PAO1$^{IF\lambda}$ strain by introducing pAY7401 *via* conjugation and selected white colonies on the X-gal plates. As shown in the Supplementary Figure S5G, selective white colonies were recovered, suggesting the successful removal of the integrated *lacZ*-containing I-F-λ_{red} cassette. Successful removal of the integrated fragment was also confirmed by PCR amplification of the region flanking the *attB* site using primer pairs P1 and P2 located upstream and downstream of the donor sequences, respectively (Figure 6A), resulting in a fragment with the desired site of 10.3 kb (Supplementary Figure S5H). The capacity of the common cassette-deleting editing plasmid was also verified by introducing pAY7401 into PAO1$^{IF\lambda}$ Δ*rhlI* cell to delete the entire mini-CTX-IF-λ_{red}-P*tat-lacZ* following curing the editing plasmid p*rhlI*-Del-1 (Supplementary Figure S5I). Colony PCR verified the successful removal of the cassette by the size of the PCR product (Figure 6B). The resulting clones were also shown to be susceptible to tetracycline, the antibiotic resistant marker in the mini-CTX-*lacZ* backbone (Supplementary Figure S5G). Meanwhile, the Δ*rhlI* genetic allele remains unchanged during the process as verified by PCR analysis. Together, these results demonstrated that the transferrable I-F-λ_{red} Cascade is capable of not only effecting diverse genetic editing in the heterologous hosts, but also being exploited to remove large-scale genomic fragments (>20 kb) with convenient selection.

DISCUSSION

Despite that class 1 CRISPR–Cas systems represent 90% of all naturally occurring CRISPR–Cas systems, their exploitations for heterologous genome editing have been hindered by the complexity of the effector Cascade. In the present study, we established a transferrable I-F Cascade based on the integration-proficient mini-CTX vector which enables integration of exogenous DNA fragments at the conserved *attB* site in diverse *Pseudomonas* genomes for stable expression and function, converting CRISPR-free cells or those containing an inactive or degenerated CRISPR–Cas system into cells with an endogenously active type I-F Cascade. Exploiting this stably expressed 'native' type I-F Cascade, efficient and precise genome editing was achieved by introducing a single editing plasmid in one step. An advanced transferrable I-F-λ_{red} Cascade is further developed to simultaneously integrate an I-F Cascade and a λ-Red recombination system in the heterologous hosts, improving genome-editing efficiency in the recipient cells with a poor intrinsic HR capacity. The transferred I-F-λ_{red} Cascade can also be harnessed for deleting large-scale genomic fragments (>20 kb) such as the entire transferred cassette, resulting in clean genetic manipulations in the genetic background of interest. Applications of the system are demonstrated in diverse genetic backgrounds, including strains with poor HR capacities, with or without native CRISPR–Cas systems, wild clinical isolates without genome sequences, as well as strains containing Acrs and other *Pseudomonas* species. To our knowledge, this is the first transferrable and integrative type I Cascade for widespread and robust heterologous genome editing. Lastly, a stable and reprogrammable 'all-in-one' I-F Cascade-based CRISPRi system was developed to provide a powerful and alternative gene knockdown strategy for functional genomics without the need of delivering additional plasmids to express the crRNA guides, further expanding the applicability of the transferrable system to a broad range of hosts with poor DNA uptake capacity and antibiotic-resistance. The

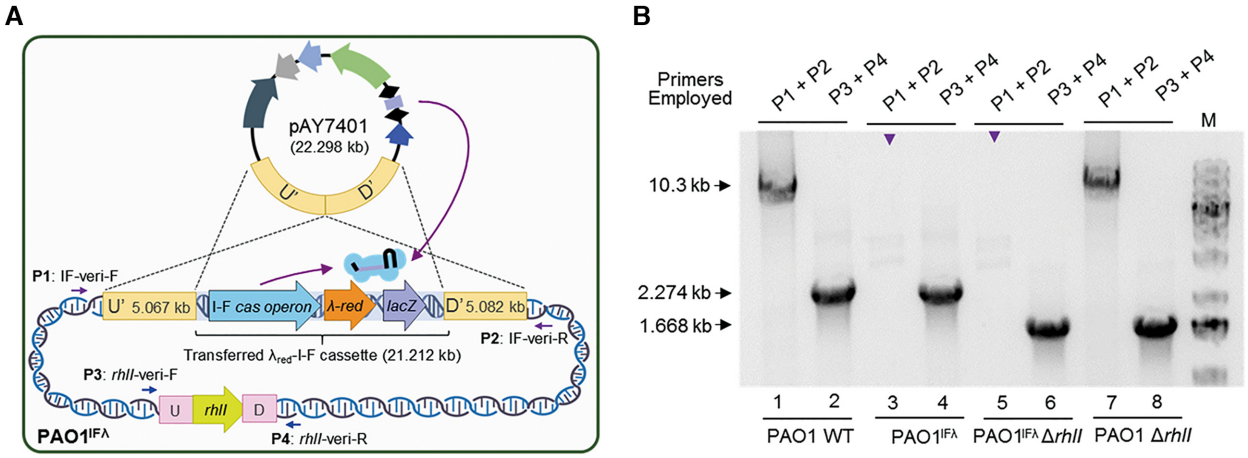

Figure 6. Transferred I-F Cascade-mediated removal of the integrated I-F-λ_{red} cassette. (**A**) Schematic diagram showing the working mechanism of deleting the transferred I-F-λ_{red} cassette by one-step transformation of a single editing plasmid pAY7401. The editing plasmid expresses a *lacZ*-targeting crRNA and provides a donor template which consists of 5.067-kb upstream (U') and 5.082-kb downstream (D') homologous arms of the *attB* site for homologous recombination. (**B**) PCR analysis to verify the desired gene editing and removal of the transferred I-F-λ_{red} cassette. Primer pairs P1 and P2 are used to verify removal of the transferred I-F-λ_{red} cassette. Primer pairs P3 and P4 are used to verify *rhlI* deletion. Presence of a 10.3-kb PCR product using the P1 and P2 primer pair indicated absence of cassette integration at the *attB* site, i.e., in the PAO1 WT and the clean edited cell PAO1 Δ*rhlI*. Absence of a PCR product using P1 and P2 primer pair indicates the presence of the integrated cassette which was incapable to be amplified by our PCR polymerase due to its large size.

methodology provides a framework to expand the diverse type I Cascades for widespread, heterologous genome editing.

The transferred I-F Cascade displayed strong DNA interference activity and efficient editing capacity in diverse genetic backgrounds. Nonetheless, false positive clones emerge following the editing reactions. Our WGS analysis showed that all three randomly selected false positive clones recovered from the editing reaction to construct Δ*rhlI* carry mutations in the *cas* genes, i.e. *cas5* and *cas2-3*. In another attempt to construct Δ*pqsA* in PAO1$^{IF\lambda}$ (data not shown), we identified false positive clones carrying mutated editing plasmid in which the spacer and the downstream repeat sequence was excised (Supplementary Figure S12), suggesting mutations in *cas* genes or the self-targeting mini-CRISPR in the editing plasmid are the major reasons for the emergence of false positive clones (55). Hence, future efforts to increase the editing efficiencies should focus on preventing these spontaneous mutations, such as modifying the repeat sequence in the mini-CRISPR to prevent the spacer excision *via* homologous recombination between the two repeats (15).

Our studies also indicated that the loci structures of protospacers being targeted affect the editing efficiency. For instance, an editing efficiency of 81.3% and 33.3% was achieved when pEditing expressing a crRNA targeting to the IF_Ps6 and IF_Ps7 site, respectively, was employed for constructing PAO1 Δ*rhlI*. These results suggest that comprehensively investigating the sequence preference of a Cascade may facilitate the selection of the most effective protospacer for genome editing. Nonetheless, we demonstrated that simultaneously targeting to multiple protospacers using a tandem mini-CRISPR is effective to prevent the inefficient targeting and editing by targeting to only one locus. Moreover, we showed that increasing the HR capacity by supplying an exogenous recombination system improved the editing efficiency in the case a relatively inefficient targeting site was employed. This capacity will be highly desirable in certain editing applications which involve limited protospacer sequence and location selections, such as site-specific gene insertion or point mutation. Notably, since the Bet recombinase of the λ-Red system favors a low GC content during the double strand DNA (dsDNA) invasion step (56), the recombineering capacity and efficiency of the λ-Red system may vary in different bacterial species displaying different GC contents. Poor recombineering capacity will be reflected by a sufficiently high self-targeting activity (conjugation efficiency of the pTargeting is 1<0.0001%) but a low editing efficiency in a strain integrated with the transferrable I-F system. This problem can be potentially solved by replacing the λ-Red system in the transferrable system, i.e. the mini-CTX-IF-λ_{red}-P*tat-lacZ* plasmid (pAY7136), with other recombinases such as RecET system derived from the *E. coli* Rac prophage and the Ssr recombinase derived from *P. putida* DOT-T1E which has been shown to be independent of GC content for dsDNA invasion activity (57–59).

Since the efficiencies of constructing *rhlI* deletion vary in different clinical strains integrated with the same I-F-λ_{red} system, it suggests that uncharacterized regulatory factors in the host may also affect the editing efficiency in addition to the recombination capacity of the host. For example, in PA14, quorum sensing (QS) was shown to regulate the expression of *cas* genes (60). However, we did not observe any significant expression changes of the transferrable *cas* genes in the recipient strain PAO1 at different growth stages (Supplementary Figure S13), suggesting that the transferred *cas* operon encoded from PA154197 is not controlled by QS systems. Nevertheless, other unidentified regulatory factors may be present and module the expression or activity of the transferred I-F system we developed which warrants further investigations.

The widely distributed anti-CRISPR elements (Acrs) are regarded as another major obstacle limiting the CRISPR–Cas-mediated genome editing, especially in the wild clinical and environmental *P. aeruginosa* isolates (20). We identified Acrs in all four wild isolates (two clinical and two environmental strains) which showed no DNA interference activity following integration of the I-F Cascade. Activities of the transferred I-F Cascade in two strains PA130788 and PA27853 were activated upon deletion of the *acr* genes and highly efficient gene deletion and robust gene repression was achieved subsequently. Thus, by combining the counter selection-based gene-deletion method to remove *acr* genes, the application of the transferred I-F Cascade can be expanded in strains containing Acrs. Although removal of *acr* genes is relatively laborious and time-consuming using conventional methods, the strategy is still advantageous as the resulting cells will enable various genetic exploitations using the transferred Cascade-based editing approach which is simple and efficient. An alternative strategy to overcome Acrs is to overexpress the anti-CRISPR-associated gene (*aca*) which represses *acr* and in turn actives CRISPR–Cas systems (61). This strategy has been demonstrated to be effective in a type I-C Cascade-mediated genome editing in a PAO1 variant which is lysogenized by a recombinant DMS3m phage expressing the anti-CRISPR gene *acrIC1* (15). However, robustness of Aca-mediated anti-anti-CRISPR strategy might be compromised in clinical strains owing to their complicated genetic backgrounds. We have applied this approach in PA130788 by overexpressing the *aca* gene of the identified *acr*. Despite that expression of *acr* was significantly repressed upon introduction of an ectopic *aca* gene and DNA interference activity of the transferred I-F Cascade was improved as shown by a conjugation efficiency of 0.5% upon introduction of pAY7138 (Supplementary Figure S14), we failed to obtain a desired Δ*rhlI* mutant after screening 960 recovered clones. Since the *acr* genes present in *P. aeruginosa* predominantly inhibit the three prevalent CRISPR–Cas subtypes I-C, I-E and I-F in this species (51), it is conceivable that developing transferrable I-A or I-B Cascade-mediated genome editing approach may overcome the barrier imposed by the common Acrs in *P. aeruginosa*.

The type II Cas9 effector has been broadly employed for genome editing in various eukaryotic and prokaryotic hosts. However, the transferrable and integrative Cas9 system failed to effect efficient self-targeting in the various recipient hosts we tested in this study. In *P. aeruginosa*, a two-plasmid-based Cas9 approach was developed to achieve efficient genome editing in PAO1 and PAK (25). By modifying the editing plasmid in the two-plasmid system to contain an origin of transfer (*oriT*), we improved the delivery efficiency of this plasmid by conjugation and successfully delivered the plasmid into PA14 and clinical strains PA151671 and PA132533. However, we found that the targeting efficiency mediated by the plasmid-borne Cas9 was still substantially lower than the transferred I-F Cascade in these strains especially in the clinical strains. This is probably due to the instability and degradation of the heterologous Cas9 protein in these cells (24). The success and ease of the transferred I-F Cascade-mediated genome editing in the clinical isolates PA151671 and PA132533 in which neither the transferred nor the plasmid-borne Cas9 effects any DNA interference clearly demonstrated the greater capacity and robustness of the transferred I-F Cascade than the Cas9 effector for heterologous genetic manipulations. Together, our studies demonstrated the power and potentials of transferrable type I Cascades for heterologous genome editing and for establishing genome editing in 'non-model' clinical and environmental isolates.

DATA AVAILABILITY

All genome data are deposited in the NCBI under the project accession number PRJNA694101 and the transcriptome sequencing result is available on FigShare at https://doi.org/10.6084/m9.figshare.13699492. The clinical strains used in this study are available on request following the export and import regulations of the sender and recipient regions.

SUPPLEMENTARY DATA

Supplementary Data are available at NAR Online.

ACKNOWLEDGEMENTS

We thank Dr Xin Deng (Department of Biomedical Sciences, City University of Hong Kong) for providing the mini-CTX-*lacZ* vector and thank Ms. Xiaojue Wang (School of Biological Sciences, The University of Hong Kong) for measurement of *cas* gene expression in the clinical strains. We thank Prof. Lian-hui Zhang (Integrative Microbiology Research Centre, South China Agricultural University) for his generous help and support during the revision of the manuscript.

FUNDING

Hong Kong University Grants Council General Research Fund [17124719 to A.Y.]; Collaborative Research Fund [C7033-20G to A.Y.]; Hong Kong Government Food and Health Bureau Health and Medical Research Fund [19180422 to A.Y.]. Funding for open access charge: Hong Kong University Grants Council General Research Fund.

Conflict of interest statement. A.Y. and Z.X. have filed a US provisional patent application (No. 63/110,683) about the transferrable I-F Cascade-based genome editing.

REFERENCES

1. Barrangou,R., Fremaux,C., Deveau,H., Richards,M., Boyaval,P., Moineau,S., Romero,D.A. and Horvath,P. (2007) CRISPR provides acquired resistance against viruses in prokaryotes. *Science*, **315**, 1709–1712.
2. Marraffini,L.A. (2015) CRISPR–Cas immunity in prokaryotes. *Nature*, **526**, 55–61.
3. Zhang,F. (2019) Development of CRISPR–Cas systems for genome editing and beyond. *Q. Rev. Biophys.*, **52**, E6.
4. Knott,G.J. and Doudna,J.A. (2018) CRISPR–Cas guides the future of genetic engineering. *Science*, **361**, 866–869.
5. Crawley,A.B., Henriksen,J.R. and Barrangou,R. (2018) CRISPRdisco: an automated pipeline for the discovery and analysis of CRISPR–Cas systems. *CRISPR J*, **1**, 171–181.
6. Vento,J.M., Crook,N. and Beisel,C.L. (2019) Barriers to genome editing with CRISPR in bacteria. *J. Ind. Microbiol. Biotechnol.*, **46**, 1327–1341.

7. Jiang,Y., Qian,F., Yang,J., Liu,Y., Dong,F., Xu,C., Sun,B., Chen,B., Xu,X., Li,Y. *et al.* (2017) CRISPR-Cpf1 assisted genome editing of *Corynebacterium glutamicum*. *Nat. Commun.*, **8**, 15179.
8. Cho,S., Choe,D., Lee,E., Kim,S.C., Palsson,B. and Cho,B.-K. (2018) High-level dCas9 expression induces abnormal cell morphology in *Escherichia coli*. *ACS Synth Biol*, **7**, 1085–1094.
9. Barrangou,R. and Marraffini,LA. (2014) CRISPR–Cas systems: prokaryotes upgrade to adaptive immunity. *Mol. Cell*, **54**, 234–244.
10. Koonin,E.V. and Makarova,K.S. (2019) Origins and evolution of CRISPR–Cas systems. *Philos. Trans. R. Soc. Lond. B Biol. Sci.*, **374**, 77.
11. Xu,Z., Li,Y., Li,M., Xiang,H. and Yan,A. (2021) Harnessing the type I CRISPR–Cas systems for genome editing in prokaryotes. *Environ. Microbiol.*, **23**, 542–558.
12. Pyne,M.E., Bruder,M.R., Moo-Young,M., Chung,D.A. and Chou,C.P. (2016) Harnessing heterologous and endogenous CRISPR–Cas machineries for efficient markerless genome editing in *Clostridium*. *Sci. Rep.*, **6**, 25666.
13. Xu,Z., Li,M., Li,Y., Cao,H., Miao,L., Xu,Z., Higuchi,Y., Yamasaki,S., Nishino,K., Woo,P. *et al.* (2019) Native CRISPR–Cas-mediated genome editing enables dissecting and sensitizing clinical multidrug-resistant *P. aeruginosa*. *Cell Rep.*, **29**, 1707–1717.
14. Hidalgo-Cantabrana,C., Goh,Y.J., Pan,M., Sanozky-Dawes,R. and Barrangou,R. (2019) Genome editing using the endogenous type I CRISPR–Cas system in *Lactobacillus crispatus*. *Proc. Natl. Acad. Sci. U.S.A.,* **116**, 15774–15783.
15. Csörgő,B., León,L.M., Chau-Ly,I.J., Vasquez-Rifo,A., Berry,J.D., Mahendra,C., Crawford,E.D., Lewis,J.D. and Bondy-Denomy,J. (2020) A compact Cascade-Cas3 system for targeted genome engineering. *Nat. Methods*, **17**, 1183–1190.
16. Dolan,A.E., Hou,Z., Xiao,Y., Gramelspacher,M.J., Heo,J., Howden,S.E., Freddolino,P.L., Ke,A. and Zhang,Y. (2019) Introducing a spectrum of long-range genomic deletions in human embryonic stem cells using type I CRISPR–Cas. *Mol. Cell*, **74**, 936–950.
17. Chen,Y., Liu,J., Zhi,S., Zheng,Q., Ma,W., Huang,J., Liu,Y., Liu,D., Liang,P. and Songyang,Z. (2020) Repurposing type I-F CRISPR–Cas system as a transcriptional activation tool in human cells. *Nat. Commun.*, **11**, 3136–3136.
18. Pickar-Oliver,A., Black,J.B., Lewis,M.M., Mutchnick,K.J., Klann,T.S., Gilcrest,K.A., Sitton,M.J., Nelson,C.E., Barrera,A., Bartelt,L.C. *et al.* (2019) Targeted transcriptional modulation with type I CRISPR–Cas systems in human cells. *Nat. Biotechnol.*, **37**, 1493–1501.
19. Stern,A., Keren,L., Wurtzel,O., Amitai,G. and Sorek,R. (2010) Self-targeting by CRISPR: gene regulation or autoimmunity? *Trends Genet.*, **26**, 335–340.
20. van Belkum,A., Soriaga,L.B., LaFave,M.C., Akella,S., Veyrieras,J.B., Barbu,E.M., Shortridge,D., Blanc,B., Hannum,G., Zambardi,G. *et al.* (2015) Phylogenetic distribution of CRISPR–Cas systems in antibiotic-resistant *Pseudomonas aeruginosa*. *Mbio*, **6**, e01796-15.
21. Hidalgo-Cantabrana,C. and Barrangou,R. (2020) Characterization and applications of type I CRISPR–Cas systems. *Biochem. Soc. Trans.*, **48**, 15–23.
22. Silby,M.W., Winstanley,C., Godfrey,S.A.C., Levy,S.B. and Jackson,R.W. (2011) *Pseudomonas genomes*: diverse and adaptable. *FEMS Microbiol. Rev.*, **35**, 652–680.
23. Brophy,J.A.N., Triassi,A.J., Adams,B.L., Renberg,R.L., Stratis-Cullum,D.N., Grossman,A.D. and Voigt,C.A. (2018) Engineered integrative and conjugative elements for efficient and inducible DNA transfer to undomesticated bacteria. *Nat Microbiol*, **3**, 1043–1053.
24. Peters,J.M., Koo,B.M., Patino,R., Heussler,G.E., Hearne,C.C., Qu,J.X., Inclan,Y.F., Hawkins,J.S., Lu,C.H.S., Silvis,M.R. *et al.* (2019) Enabling genetic analysis of diverse bacteria with Mobile-CRISPRi. *Nat Microbiol*, **4**, 244–250.
25. Chen,W., Zhang,Y., Zhang,Y., Pi,Y., Gu,T., Song,L., Wang,Y. and Ji,Q. (2018) CRISPR/Cas9-based genome editing in *Pseudomonas aeruginosa* and cytidine deaminase-mediated base editing in *Pseudomonas* species. *iScience*, **6**, 222–231.
26. Xu,Z., Wang,P., Wang,H., Yu,Z., Au-Yeung,H., Hirayama,T., Sun,H. and Yan,A. (2019) Zinc excess increases cellular demand for iron and decreases tolerance to copper in *Escherichia coli*. *J. Biol. Chem.*, **294**, 16978–16991.
27. Schmittgen,T.D. and Livak,K.J. (2008) Analyzing real-time PCR data by the comparative CT method. *Nat. Protoc.*, **3**, 1101–1108.
28. Xu,Z., Li,Y. and Yan,A. (2020) Repurposing the native type I-F CRISPR–Cas system in *Pseudomonas aeruginosa* for genome editing. *STAR Protoc*, **1**, 100039.
29. Volke,D.C., Friis,L., Wirth,N.T., Turlin,J. and Nikel,P.I. (2020) Synthetic control of plasmid replication enables target- and self-curing of vectors and expedites genome engineering of *Pseudomonas putida*. *Metab Eng Commun*, **10**, e00126.
30. Bolger,A.M., Lohse,M. and Usadel,B. (2014) Trimmomatic: a flexible trimmer for illumina sequence data. *Bioinformatics*, **30**, 2114–2120.
31. Bankevich,A., Nurk,S., Antipov,D., Gurevich,A.A., Dvorkin,M., Kulikov,A.S., Lesin,V.M., Nikolenko,S.I., Pham,S., Prjibelski,A.D. *et al.* (2012) SPAdes: A new genome assembly algorithm and its applications to single-cell sequencing. *J. Comput. Biol.*, **19**, 455–477.
32. Page,A.J., De Silva,N., Hunt,M., Quail,M.A., Parkhill,J., Harris,S.R., Otto,T.D. and Keane,J.A. (2016) Robust high-throughput prokaryote de novo assembly and improvement pipeline for illumina data. *Microb Genom*, **2**, e000083.
33. Hunt,M., Silva,N.D., Otto,T.D., Parkhill,J., Keane,J.A. and Harris,S.R. (2015) Circlator: automated circularization of genome assemblies using long sequencing reads. *Genome Biol.*, **16**, 294.
34. Seemann,T. (2014) Prokka: rapid prokaryotic genome annotation. *Bioinformatics*, **30**, 2068–2069.
35. Klompe,S.E., Vo,P.L.H., Halpin-Healy,T.S. and Sternberg,S.H. (2019) Transposon-encoded CRISPR–Cas systems direct RNA-guided DNA integration. *Nature*, **571**, 219–225.
36. Li,H., Handsaker,B., Wysoker,A., Fennell,T., Ruan,J., Homer,N., Marth,G., Abecasis,G. and Durbin,R. (2009) The sequence alignment/map format and SAMtools. *Bioinformatics*, **25**, 2078–2079.
37. Quinlan,A.R. and Hall,I.M. (2010) BEDTools: a flexible suite of utilities for comparing genomic features. *Bioinformatics*, **26**, 841–842.
38. Cao,H., Xia,T., Li,Y., Xu,Z., Bougouffa,S., Lo,Y., Bajic,V., Luo,H., Woo,P. and Yan,A. (2019) Uncoupled quorum sensing modulates the interplay of virulence and resistance in a multidrug-resistant clinical*Pseudomonas aeruginosa* isolate belonging to the MLST550 clonal complex. *Antimicrob. Agents Chemother.*, **63**, e01944-18.
39. Richter,C., Gristwood,T., Clulow,J.S. and Fineran,P.C. (2012) In vivo protein interactions and complex formation in the *Pectobacterium atrosepticum* subtype I-F CRISPR/Cas System. *PLoS One*, **7**, e49549.
40. Rollins,M.F., Chowdhury,S., Carter,J., Golden,S.M., Wilkinson,R.A., Bondy-Denomy,J., Lander,G.C. and Wiedenheft,B. (2017) Cas1 and the Csy complex are opposing regulators of Cas2/3 nuclease activity. *Proc. Natl. Acad. Sci. U.S.A.*, **114**, E5113–E5121.
41. Becher,A. and Schweizer,H.P. (2000) Integration-proficient *Pseudomonas aeruginosa* vectors for isolation of single-copy chromosomal *lacZ* and *lux* gene fusions. *BioTechniques*, **29**, 948–950.
42. Shah,N. and Naseby,D.C. (2014) Bioluminescence-based measurement of viability of *Pseudomonas aeruginosa* ATCC 9027 harbouring plasmid-based *lux* genes under the control of constitutive promoters. *J. Appl. Microbiol.*, **117**, 1373–1387.
43. Leenay,R.T. and Beisel,C.L. (2017) Deciphering, communicating, and engineering the CRISPR PAM. *J. Mol. Biol.*, **429**, 177–191.
44. Duan,K. and Surette,M.G. (2007) Environmental regulation of *Pseudomonas aeruginosa* PAO1 *las* and *rhl* quorum-sensing systems. *J. Bacteriol.*, **189**, 4827–4836.
45. Gudbergsdottir,S., Deng,L., Chen,Z., Jensen,J.V.K., Jensen,L.R., She,Q. and Garrett,R.A. (2011) Dynamic properties of the Sulfolobus CRISPR/Cas and CRISPR/Cmr systems when challenged with vector-borne viral and plasmid genes and protospacers. *Mol. Microbiol.*, **79**, 35–49.
46. Stout,E.A., Sanozky-Dawes,R., Goh,Y.J., Crawley,A.B., Klaenhammer,T.R. and Barrangou,R. (2018) Deletion-based escape of CRISPR–Cas9 targeting in Lactobacillus gasseri. *Microbiology*, **164**, 1098–1111.
47. Walker,J.E., Lanahan,A.A., Zheng,T., Toruno,C., Lynd,L.R., Cameron,J.C., Olson,D.G. and Eckert,C.A. (2020) Development of both type I–B and type II CRISPR/Cas genome editing systems in the cellulolytic bacterium *Clostridium thermocellum*. *Metab. Eng. Commun.*, **10**, e00116.

48. Rodríguez-Beltrán,J., Tourret,J., Tenaillon,O., López,E., Bourdelier,E., Costas,C., Matic,I., Denamur,E. and Blázquez,J. (2015) High recombinant frequency in extraintestinal pathogenic *Escherichia coli* strains. *Mol. Biol. Evol.*, **32**, 1708–1716.
49. Couvin,D., Bernheim,A., Toffano-Nioche,C., Touchon,M., Michalik,J., Néron,B., Rocha,E.P.C., Vergnaud,G., Gautheret,D. and Pourcel,C. (2018) CRISPRCasFinder, an update of CRISRFinder, includes a portable version, enhanced performance and integrates search for Cas proteins. *Nucleic Acids Res.*, **46**, W246–W251.
50. Peng,X., Mayo-Muñoz,D., Bhoobalan-Chitty,Y. and Martínez-Álvarez,L. (2020) Anti-CRISPR proteins in archaea. *Trends Microbiol.*, **28**, 913–921.
51. Marino,N.D., Pinilla-Redondo,R., Csorgo,B. and Bondy-Denomy,J. (2020) Anti-CRISPR protein applications: natural brakes for CRISPR–Cas technologies. *Nat. Methods*, **17**, 471–479.
52. Yi,H., Huang,L., Yang,B., Gomez,J., Zhang,H. and Yin,Y. (2020) AcrFinder: genome mining anti-CRISPR operons in prokaryotes and their viruses. *Nucleic. Acids. Res.*, **48**, W358–W365.
53. Choi,K.H. and Schweizer,H.P. (2005) An improved method for rapid generation of unmarked *Pseudomonas aeruginosa* deletion mutants. *BMC Microbiol.*, **5**, 30.
54. Bikard,D., Jiang,W., Samai,P., Hochschild,A., Zhang,F. and Marraffini,L.A. (2013) Programmable repression and activation of bacterial gene expression using an engineered CRISPR–Cas system. *Nucleic. Acids. Res.*, **41**, 7429–7437.
55. Selle,K. and Barrangou,R. (2015) Harnessing CRISPR–Cas systems for bacterial genome editing. *Trends Microbiol.*, **23**, 225–232.
56. Rybalchenko,N., Golub,E.I., Bi,B. and Radding,C.M. (2004) Strand invasion promoted by recombination protein β of coliphage λ. *Proc. Natl. Acad. Sci. U.S.A.*, **101**, 17056–17060.
57. Noirot,P. and Kolodner,R.D. (1998) DNA strand invasion promoted by *Escherichia coli* RecT protein. *J. Biol. Chem.*, **273**, 12274–12280.
58. Aparicio,T., Jensen,S.I., Nielsen,A.T., de Lorenzo,V. and Martínez-García,E. (2016) The Ssr protein (T1E_1405) from *Pseudomonas putida* DOT-T1E enables oligonucleotide-based recombineering in platform strain *P. putida* EM42. *Biotechnol. J.*, **11**, 1309–1319.
59. Choi,K.R., Cho,J.S., Cho,I.J., Park,D. and Lee,S.Y. (2018) Markerless gene knockout and integration to express heterologous biosynthetic gene clusters in *Pseudomonas putida*. *Metab. Eng.*, **47**, 463–474.
60. Høyland-Kroghsbo,N., Paczkowski,J., Mukherjee,S., Broniewski,J., Westra,E., Bondy-Denomy,J. and Bassler,B.L. (2017) Quorum sensing controls the *Pseudomonas aeruginosa* CRISPR–Cas adaptive immune system. *Proc. Natl. Acad. Sci. U.S.A.*, **114**, 131–135.
61. Stanley,S.Y., Borges,A.L., Chen,K.H., Swaney,D.L., Krogan,N.J., Bondy-Denomy,J. and Davidson,A.R. (2019) Anti-CRISPR-associated proteins are crucial repressors of anti-CRISPR transcription. *Cell*, **178**, 1452–1464.